Dynamics of entangled metallo-supramolecular polymer networks combining stickers with different lifetimes

Yanzhao Li[1], Christina Pyromali[2,3], Flanco Zhuge[1], Charles-André Fustin[1], Jean-François Gohy[1], Dimitris Vlassopoulos[2,3], Evelyne van Ruymbeke[1]

1. Bio- and Soft Matter (BSMA), Institute of Condensed Matter and Nanosciences, Université catholique de Louvain, Croix du Sud 1, Louvain-la-Neuve B-1348, Belgium

2. Institute of Electronic Structure and Laser, FORTH, Heraklion 71110, Crete, Greece

3. Department of Materials Science & Technology, University of Crete, Heraklion 71003, Crete, Greece

ABSTRACT:

We study the linear viscoelastic properties of polymeric networks formed by poly(n-butyl acrylate) telechelic stars end-capped with 2,2:6,2''-terpyridine (Star-PnBA-tpy4) and two types of metal-ligand crosslinks with different lifetimes. The influence of interactions, mediated by temperature, nature of metal ions and ion content, on the linear viscoelastic behavior of both single and double dynamics transient networks is systematically investigated by small amplitude oscillatory shear and creep rheometry. The experimental results reveal that the dynamics of networks with two different metal-ligand crosslinks is much faster than expected, characterized by the average sticker lifetime rather than a discrete contribution of each metal-ligand complex. We model the dynamics with the help of our modified tube-based time marching algorithm (TMA) by accounting for both association/dissociation

dynamics of metal-ligand coordination and the entanglement dynamics. Two parameters are defined in the model, namely, the proportion of dangling ends and the average time during which a sticker is free. This allows us to quantify the transient dynamics of the network, and in particular to determine how the sticker dynamics depend on temperature and ion content.

I. INTRODUCTION

The use of supramolecular interactions including metal-ligand coordination[1-6], hydrogen bonding[7-9], ionic[10,11] and hydrophobic interactions[12,13] plays an important role for the rational design of polymeric materials with desired properties. However, this requires first to understand the underlying relationship between supramolecular dynamics and bulk material properties. To this end, a variety of functionalized polymeric building blocks has been used to create polymeric self-assemblies[14-16] or transient networks, including telechelic linear or star building blocks and polymer chains with pendant groups along their backbone, i.e., sticky chains. In these materials, the lifetime of supramolecular junctions can be controlled in several ways, for example by adjusting the nature of the reversible junctions or of the metal ion in case of metal-ligand coordination, using a mixture of multiple physical crosslinks within the material as well as altering external conditions, such as temperature, solvent and pH, to finely modulate the sample properties. It has been shown that the dynamic nature of reversible interactions is central to the mechanical properties of associating polymers, since it controls the evolution of structure and viscoelasticity in response to environmental changes. This is illustrated, for example, in the work of Mozhdehi et al.,[17] who showed that it is possible to simultaneously control the coordination geometry, the topology of the networks and the time response of imidazole-containing polymers by using dynamic associations of weak mono-dentate ligands with either Co(II) or Zn(II) or Cu(II) ions. In particular, the authors showed that the mechanical properties of these transient networks are correlated with the ratio of metal ions to ligand, as well as the presence of unbound free ligands.[17]

Since the properties of supramolecular polymeric networks depend greatly on the stickers, a new strategy has emerged recently, which consists in utilizing multiple noncovalent interactions to tailor their viscoelasticity. In this direction, Loveless et al. combined different Pd(II) and Pt(II) organometallic crosslinkers within a poly(4-vinylpyridine) polymer, and obtained a material with distinct individual contributions of each type of cross-linker to its viscoelastic properties, rather than an average of the contributing species.[18,19] Guillet et al. introduced a strategy combining block copolymers and metal-ligand associations to engineer highly tunable and hierarchical supramolecular networks.[20] Similarly, Brassinne et al. reported on the combination of hydrophobic interaction and metal-ligand coordination through the synthesis of terpyridine end-functionalized polystyrene-*block*-poly-(*N*-isopropylacrylamide) block copolymers. In the latter approach, discrete linear responses and multistep yielding were observed by varying metal ion nature and the length of hydrophobic segments.[21] Nair et al. reported on the synthesis of side-chain-functionalized polymers using both hydrogen bonding and metal-ligand interactions to obtain multi-responsive networks exhibiting both thermo- and chemo-responsiveness. In this work, ligand displacement agents were selectively utilized to de-crosslink either the hydrogen bond physical crosslinks or the metal-ligand coordination, respectively.[22] Narita et al. studied the dynamics of double crosslinked poly(vinyl alcohol) (PVA) gels which combine chemical and physical crosslinks. They showed that these systems display peculiar dynamics at intermediate frequencies, characterized by $G'=G''\sim\omega^{0.5}$, providing evidence of an associative Rouse mode governed by the association dynamics of the reversible PVA-borate ion complexation in this chemically crosslinked hydrogel.[23] Similar behavior was observed by Yang et al.[24], who studied the viscoelastic properties of interpenetrated transient polymer networks with different lifetimes, due to the different nature of the supramolecular junctions. Grindy et al. tuned the dynamics of a 4-arm poly(ethylene glycol) end-functionalized with a histidine moiety (4PEG-His) by incorporating two different pairs of metal ions, either Ni(II)/Zn(II) or Ni(II)/Cu(II), into the telechelic star polymer. By varying the ratio of the two transient crosslinks, multiple energy-dissipating behavior

was obtained.[25] In addition, many studies focused on enhancing macroscopic properties of double crosslinked systems including self-healing, shape memory, toughness, stretchability and resistance to fatigue.[26-28]

Thus, the use of diverse but highly specific crosslinking dynamics has been shown to provide a means to engineer materials with complex viscoelastic behaviors and mechanical properties. To build these transient networks, metal−ligand crosslinks are particularly interesting since they offer a suitable way to tune both structural and temporal parameters by careful selection of the ligand and the metal ions without significant synthetic modifications of the polymer backbone. Most of the above-mentioned investigations concerned double dynamics networks which were unentangled and examined in solution. Furthermore, the majority of those works were conducted with a stoichiometric amount of ions. However, as concluded by Mozhdehi et al.[17], the presence of unassociated ligands in the material can also play a critical role in the viscoelastic response of the material as they can accelerate the stress relaxation by ligand exchange mechanism. Therefore, by varying the ion content, the fraction of dangling ends is expected to vary, which should influence the stress relaxation of the transient network. In the present work, we shall quantify the proportion of dangling ends as function of the amount of metal ions, and rationalize their influence on the relaxation of the transient network.

As the dynamics of the noncovalent interactions is controlled by the thermodynamics and kinetic parameters, equilibrium binding constants of the metal-ligand complexes can be used to explain the formation of the supramolecular junctions. For example, Grindy et al. estimate the concentration of Histidine: Ni^{2+} complexes with increasing ion content based on the corresponding equilibrium constants, which is correlated with the static elasticity of the resulting tetra-arm poly(ethylene glycol) hydrogels.[29] Another example are the works of Fullenkamp et al.[30] and Cazzell et al.[31], where the equilibrium constants as function of pH were used to determine the concentration of each species in

hydrogels networks. However, it is not straightforward to relate the equilibrium constants in solution to the viscoelastic behavior of the resulting polymer networks in the melt. Moreover, when two metal ions are used to create a double dynamics network, assessing their relative priority to coordinate with a ligand represents a challenge. This is presently not fully understood on the basis of simple thermodynamic and kinetic arguments related to the metal ligand complexes, especially when the ions are added in excess. Another parameter which may influence the dynamics of the supramolecular interactions is the mobility of the building blocks, i.e., their ability to diffuse and create new supramolecular junctions.[30,32] In particular, if the building blocks are long and entangled, their diffusion is strongly slowed down, which may significantly affect the properties of the transient network.[33] Therefore, understanding the interplay between entanglements and supramolecular dynamics is of prime importance.

The goal of the present work is to address the above challenges by systematically investigating the dynamics of metallo-supramolecular networks built from entangled telechelic star polymers, and determining the influence of two different metal ions in the network. We expect to improve our ability to tune the dynamics of such complex transient networks and also understand the interplay of dynamics of stickers and entanglements.

Our supramolecular system comprises entangled telechelic poly(n-butyl acrylate) stars end-capped with 2,2:6,2''-terpyridine at each chain(arm) extremity (Star-PnBA-tpy4). Their synthesis has been described in a previous study.[34,35] In order to form tpy-M^{2+} complexes, divalent transition metal ions are added. Here, the single/double dynamic networks of Star-PnBA-tpy4 are built via adding Cu(II) and/or Zn(II). The linear viscoelastic behavior of single- and double- dynamics networks is systematically investigated by small amplitude oscillatory shear measurements, complemented by creep measurement where needed, at different temperatures, ion type and ion content. The synergistic effect of entanglement dynamics and association/dissociation events of the metal-ligand complexes is

assessed. To this end, we modify our TMA (time marching algorithm)[36,37] tube model, in order to account for these different dynamics.

II. EXPERIMENTAL SECTION

Materials. Terpyridine end-functionalized telechelic four-arm stars (M_n=249kg/mol, PDI=1.2) were synthesized via reversible addition-fragmentation chain-transfer (RAFT) polymerization in bulk conditions.[34,35] Their glass transition temperature is around -52°C.[34] The number of the entanglement per arm is 3.4, which is calculated with M_e=18kg/mol. The chemical structure on the precursor sample is given in Figure 1.a.

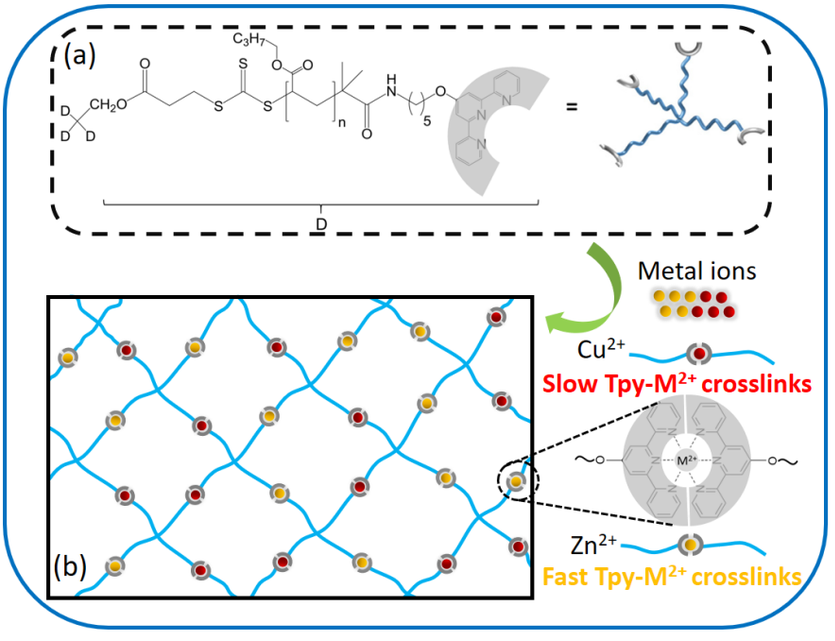

Figure 1. (a) Chemical structure of four-arm telechelic PnBA star end-functionalized with terpyridine, and (b) Schematic representation of an ideal metal-ligand transient double dynamics networks. Note that Cl^- anions which are present to neutralize the charges are purposely not represented for the clarity of the scheme.

Metal Incorporation. To obtain the metallo-supramolecular networks, pre-determined amounts of star polymer and $ZnCl_2$ and $CuCl_2$ were separately dissolved in acetone or methanol to obtain

homogeneous concentrated solutions. The concentration of the metal ion solution is ranging from 5g/L to 20g/L depending on samples with different amount of metal ions. Subsequently, the metallo-supramolecular polymer with single-metal ions was readily obtained by adding required volume of the metal salt solution to the polymeric solution to reach a final concentration of 500g/L, where the amount of metal ions was varied from half an equivalent compared to the terpyridine ligands (0.5eq., i.e., at stoichiometric conditions, where one metal ion coordinated with two ligands) to excess content. The solutions in the closed vials were stirred at least for half an hour and kept at room temperature to ensure sufficient complexation. The bulk single dynamic networks were obtained by evaporating the solvent with a rotavapor, and keeping the samples in a vacuum oven at 40°C for at least 24h. On the other hand, double dynamics networks were prepared by evenly mixing given amounts of respective single-metal ion (Zn(II) or Cu(II)) networks, which were dissolved in acetone at a concentration of 500g/L. The reaction vials were again shaken and left at room temperature for at least an hour. The solvent was then removed as described above and the sample was kept in a vacuum oven at 40°C. The molar amount of Zn(II) is nearly equal to that of its Cu(II) counterpart in double dynamics networks due to the fact that the molecular weight of $ZnCl_2$ (136.286 g/mol) is close to that of $CuCl_2$ (134.45 g/mol). The composition of the various samples is listed in Table 1. Hereafter, we use the following nomenclature: polymer−metal−M/L ratio. For example, Star250k-Zn-0.5eq. refers to the single dynamic polymer network where the telechelic star PnBA is coordinated with half an equivalent Zn(II), i.e., one zinc ion has been added for two terpyridine ligands. Likewise, Star250k-ZnCu-1.0eq. corresponds to the double dynamics networks where the telechelic star PnBA are simultaneously crosslinked with Zn(II) and Cu(II) at a ratio of one zinc ion and one copper ion over two terpyridine ligands.

Table 1. List of investigated samples

Sample	Description

Star250k-Reference	Precursor sample without metal ions
Star250k-Zn-0.5eq.	Single dynamic network with 0.5eq. Zn(II)
Star250k-Zn-0.75eq.	Single dynamic network with 0.75eq. Zn(II)
Star250k-Zn-1.0eq.	Single dynamic network with 1.0eq. Zn(II)
Star250k-Zn-1.25eq.	Single dynamic network with 1.25eq. Zn(II)
Star250k-Cu-0.5eq.	Single dynamic network with 0.5eq. Cu(II)
Star250k-Cu-0.75eq.	Single dynamic network with 0.75eq. Cu(II)
Star250k-Cu-1.0eq.	Single dynamic network with 1.0eq. Cu(II)
Star250k-Cu-1.25eq.	Single dynamic network with 1.25eq. Cu(II)
Star250k-ZnCu-0.5eq.	Double dynamics network with 0.25eq. Zn(II) and 0.25eq.Cu(II)
Star250k-ZnCu-0.75eq.	Double dynamics network with 0.375eq. Zn(II) and 0.375eq.Cu(II)
Star250k-ZnCu-1.0eq.	Double dynamics network with 0.5eq. Zn(II) and 0.5eq.Cu(II)

Rheological Characterization. Small amplitude oscillatory shear (SAOS) measurements were carried out by using an ARES-2KFRTN1 (TA Instruments) and a MCR-301 (Anton Paar) rheometers. Samples were placed between stainless steel parallel plates (diameter of 8 mm) with varying thickness between 300 and 500μm. The samples were equilibrated on the rheometer at 130°C for 30 min under nitrogen atmosphere, and normal forces were checked to be relaxed prior to any measurement. Dynamic frequency sweep measurements were performed over a wide temperature range from -20 to 100°C (-20, 0, 25, 40, 60, 80 and 100°C). At each temperature, the equilibration of the samples was checked with dynamic time sweep measurements. All dynamic measurements were performed in the linear viscoelastic region, which was determined from dynamic strain sweep tests. For the slowly relaxing samples, the low-frequency regimes were extended by means of creep measurements. The equilibrated material was subjected to a constant shear stress using the MCR-702 (Anton Paar) rheometer operating in stress-controlled mode. The time-dependent creep compliance, J(t), in the linear regime was obtained[38]. The conversion of creep data to dynamic response was performed with NLReg application that is based on generalized Tikhonov regularization for constraining the nonlinear regressions[39].

The frequency-dependent dynamic moduli were combined onto master curves at a reference temperature of 25°C using the time-temperature superposition (TTS) principle. A vertical shift was applied in order to compensate for the density variation. The vertical shift factors, b_T, were expressed as $b_T=\rho(T_{ref})T_{ref}/\rho(T)T$, where $\rho(T)$ is the density (g/cm^3) of the PnBA at temperature T(K), and the reference temperature T_{ref}=298.15K. In the case of PnBA, the temperature (T) dependence of the density is given by $\rho(T)=1.2571-6.89x10^{-4}T$.[40,41] Then, the data were shifted horizontally along the frequency axis and the horizontal shift factor, a_T, was determined based on Star250k reference sample. By best-fitting a_T values with the Williams–Landel–Ferry(WLF) equation, $\log a_T=-C_1(T-T_{ref})/(C_2+T-T_{ref})$, the constants C_1=6.2 and C_2=131.17K are obtained, as shown in Figure 2.b. In this way, the master curves of metallo-supramolecular polymers were constructed based on shift factors, a_T and b_T, of the Star250k-Reference sample.

Fourier-Transform Infrared Spectroscopy (FTIR). FT-IR spectra were obtained for all samples by using a Nicolet Nexus 8700 FTIR spectrometer. The viscoelastic samples were loaded on a KRS-5 plate and the spectra were recorded using transmission mode method at room temperature in the range 400-4000 cm^{-1} with a resolution of 4cm^{-1} with 64 scans. The resulting spectra were normalized based on Star250k-Reference sample for analysis.

III. MODELING OF THE LINEAR VISCOELASTICITY

In this section, we first briefly review the tube-based Time Marching Algorithm (TMA) model that predicts the viscoelastic behavior of entangled homopolymers. We focus here on star architectures. Further details can be found in previous works reported in the literature [36,37]. Then, we modify this model and apply it to the present case, i.e., telechelic, moderately entangled star molecules. In order to keep the model as simple as possible, the star molecules have been considered as monodisperse.

III.1. TMA model for entangled homopolymer stars

In order to determine the storage and loss moduli of a monodisperse star polymer, we first calculate its relaxation modulus as a function of time, $G(t)$, which can be transformed into the complex (storage and loss) moduli by Fourier transformation or by using the formula of Schwarzl.[42] The relaxation modulus accounts for both the high-frequency Rouse process, $G_R(t)$, and the disentanglement modulus, $G_d(t)$. While $G_R(t)$ describes the local rearrangement of chain segments between two successive entanglements, $G_d(t)$ describes the disentanglement process of the star arms, so that the total stress relaxation becomes:

$$G(t) = G_{\mathrm{R}}(t) + G_{\mathrm{d}}(t) \tag{1}$$

with

$$G_R(t) = \frac{\rho RT}{M_{arm}} \left\{ \frac{1}{4} \sum_{p=1}^{Z} exp\left(-\frac{p^2 t}{\tau_R(M_{arm})} \right) + \sum_{p=Z+1}^{n} exp\left(-\frac{2p^2 t}{\tau_R(M_{arm})} \right) \right\}. \tag{2}$$

In Equation 2, Z is the number of entanglements per arm, $Z=M_{arm}/M_e$, with M_e being the average molar mass of an entanglement segment, while $\tau_R(M_{arm})$ represents the Rouse time associated to an arm of the star and is equal to $\tau_e Z^2$ with τ_e being the Rouse time of an entanglement segment. The parameter ρ is the monomeric density and R is the gas constant.

The disentanglement modulus and the plateau modulus G_N^0 are defined as:

$$G_d(t) = G_N^0 \varphi(t) \{\phi(t)\}^{\alpha} \quad , \tag{3}$$

$$G_N^0 = \frac{4}{5} \frac{\rho RT}{M_e}, \tag{4}$$

where $\varphi(t)$ represents the unrelaxed fraction of initial tube segments and α the dynamic dilution exponent, which is fixed to 1 here. Constraint release (CR) mechanisms are taken into account by the dilution factor $\phi(t)$, which defines the diameter a of the dilated tube ($a = a_0 \cdot \phi(t)^{-\alpha/2}$, with a_0, the initial tube diameter). For a monodisperse sample, $\phi(t)$ represents the unrelaxed fraction of initial tube

segments $\varphi(t)$. The latter is calculated by considering all molecular segments x along a representative arm, ranging from $x = 0$ at its extremity to $x = 1$ at the branching point, and determining whether they are still moving or not in their initial tube:

$$\varphi(t) = \int_0^1 p_{fluc}(x,t) \quad dx. \tag{5}$$

In this equation, $p_{fluc}(x,t)$ is the survival probability of the segment x related to the (arm) fluctuation process. It is equal to $exp(-t/\tau_{fluc}(x))$, where the fluctuation time $\tau_{fluc}(x)$ is the time needed for a molecular segment x to relax by taking into account both early fluctuations of the chain ends, and deeper, activated, retraction of the arms:

$$\tau_{early}(x) = \frac{9\pi^3}{16}\tau_e \left(\frac{M_{arm}}{M_e}\right)^4 x^4 \tag{6.a}$$

$$ln\,\tau_{activated}\,(x) = ln\,\tau_{activated}\,(x-\delta x) + 3\left(\frac{M_{arm}}{M_e}\right) x\,\phi(x)^{\alpha}\,(\delta x) \tag{6.b}$$

The transition between these two processes takes place at the segment x_{tr} where the retraction potential ($U(x_{tr})=kT\,ln(\tau_{activated}(x_{tr}))$ becomes equal to kT:

$$\tau_{fluc}(x) = \tau_{early}(x) \qquad \text{for } x \le x_{tr} \tag{7.a}$$

$$\tau_{fluc}(x) = \tau_{early}(x_{tr}) \quad exp\left(\frac{\tau_{activated}(x)}{\tau_{activated}(x_{tr})}\right) \qquad \text{for } x > x_{tr} \tag{7.b}$$

In Equation 6.b, it is considered that the molecular segment located just before the segment x is positioned at $(x-\delta x)$. The function $\phi(x)$ represents the polymer fraction which has not relaxed at the time the segment x of the arm is relaxing. It is equal to $(1-x)$ for monodisperse samples.

This model is using three material parameters, namely G_N^0, M_e and τ_e. Their respective values have been determined to be 175kPa, 18kg/mol and 3.3x10^{-4}s, very similar to the values used in ref. [35] for PnBA. A comparison between the predictions obtained with the TMA model and the experimental data of the reference sample (without metal ions) is depicted in Figure 2.a, along with the shift factors used to build the linear viscoelastic master curve at a reference temperature of 25°C.

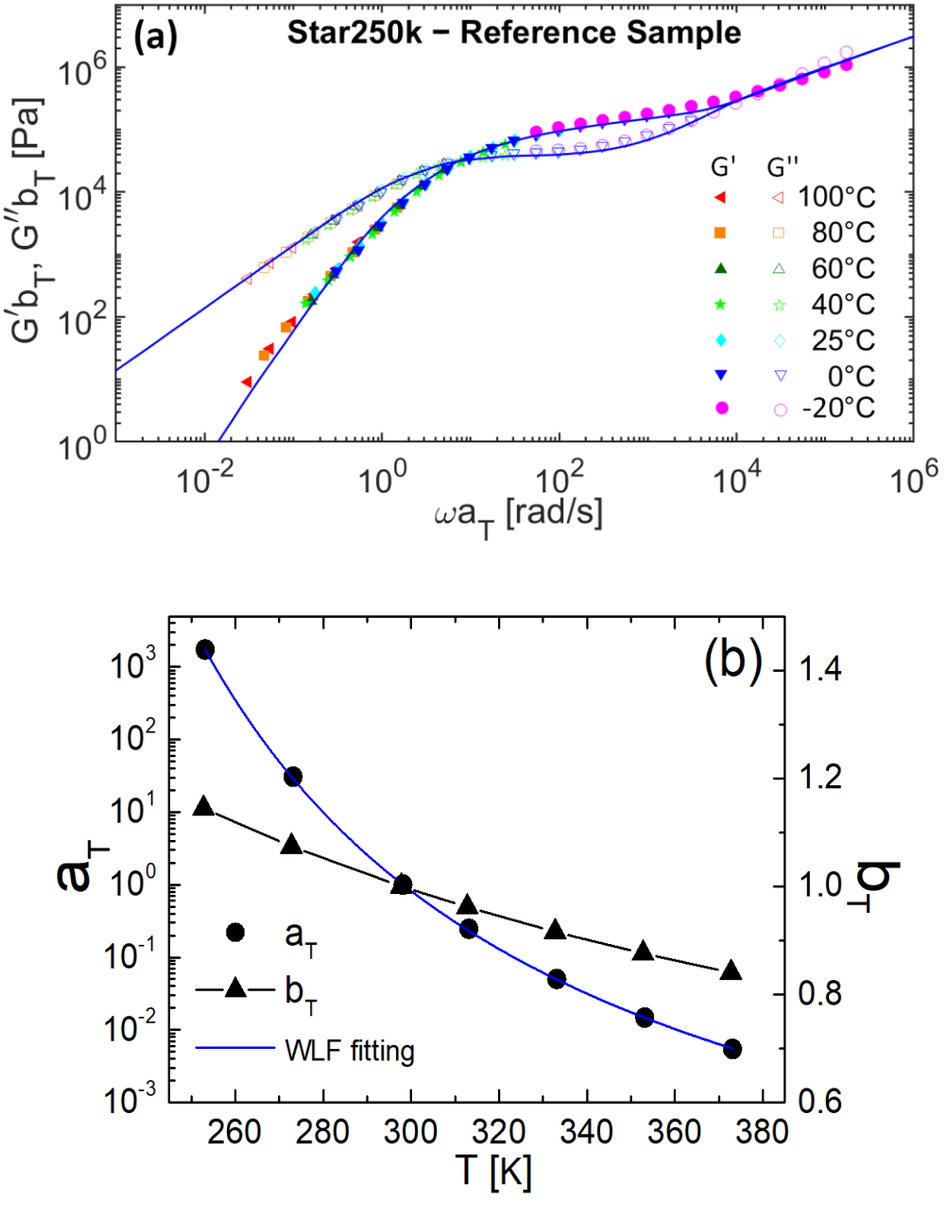

Figure 2. (a) Shifted frequency dependent storage and loss moduli of sample Star250k-Reference as functions of the shifted frequency. The storage modulus G' is represented by filled symbols and the loss modulus G'' by empty symbols. The data

have been shifted to the reference temperature of 25°C, based on the shift factors (see Section II) shown in (b). The continuous curves in(a) represent the predictions obtained with the original TMA model described by Equations 1-7.

III.2. TMA model for telechelic star molecules

As discussed in Section IV, the main effect of the stickers is to induce an overall delay of the star arm relaxation, i.e., the stickers are acting as an extra friction points located at the arms extremities, which slow-down the overall arm retraction process. This is taken into account in the model by considering that the star arms can effectively relax only during a fraction p_{free} of the total time t, i.e., they can only diffuse and disentangle during the time $(p_{free}t)$ when their end groups remain dissociated. Furthermore, as mentioned in the Introduction, it is expected that there is a certain fraction of arms which do not participate in the transient network, either because they are not functionalized, or because there is no free ion in their surroundings. Therefore, in the model, this fraction of dangling arms, which is called p_{dang}, must be accounted for. We consider that these free arms relax at short times, similarly to the arms of the reference sample. Consequently, the survival probability of a molecular segment x of a star arm becomes:

$$p_{fluc}(x,t) = p_{dang}\, exp\left(\frac{-t}{\tau_{fluc}(x)}\right) + (1 - p_{dang})\, exp\left(\frac{-p_{free}\, t}{\tau_{fluc}(x)}\right). \quad (8)$$

Thus, to account for the influence of stickers, two new parameters are introduced, p_{dang} and p_{free}. They are first considered as fit parameters and their respective values are easily determined from the experimental data. Then, in Section IV.3., the best-fit values are analyzed in detail, in order to rationalize the viscoelastic behavior of the transient networks.

In this approach, we do not consider intra-molecular associations explicitly. Since the sample elasticity is governed by the entanglements, which are also present in case of intra-molecular associations, we do not expect that this assumption affects our overall analysis.

IV. RESULTS AND DISCUSSION

The linear viscoelastic properties of terpyridine end-functionalized metallo-supramolecular polymer networks strongly depend on the metal-ligand exchange kinetics, which may vary by several orders of magnitude in time, depending on the ion type, ion content and temperature. In this section, we systematically investigate single- and double dynamics networks by small amplitude oscillatory shear measurements and analyze the results with our modified TMA model in order to quantify the influence of both entanglement and dissociation dynamics of the metal-ligand complexes, as well as to understand the competition of the two distinct metal-ligand dynamics in the double dynamics networks.

IV.1. Single dynamic networks

A. Influence of the ion type. In order to explore the influence of the metal-ligand complexes on the rheological behavior of the networks, we first vary the type of the ions added to the telechelic star polymer. To this end, stars containing a small excess, i.e., 0.75eq. of metal ion with respect to ligand (rather than stoichiometric amount), have been investigated. Indeed, as discussed below, a significant fraction of dangling ends is still present at 0.5eq. of metal ions (stoichiometric equivalent). Using a slightly larger amount of metal ion reduces their presence and promotes metal-ligand association. The viscoelastic data of Star250k-Zn-0.75eq. and Star250k-Cu-0.75eq. at 40°C are shown in Figure 3, in comparison with the data of the reference sample.

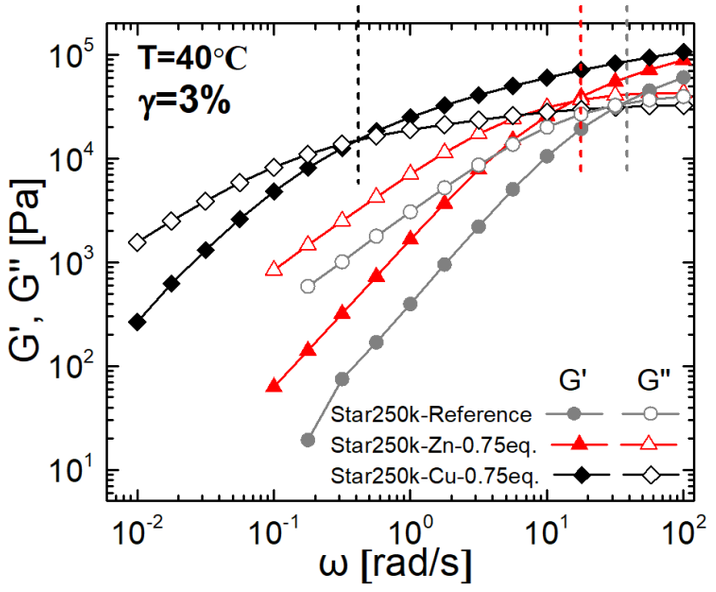

Figure 3. Storage and loss moduli of Star250k-Zn-0.75eq. and Star250k-Cu-0.75eq. as functions of angular frequency at 40°C. The grey circles correspond to Star250k-Reference (without metal ions). The storage modulus G' is represented by filled symbols and the loss modulus G'' by empty symbols. The dashed lines mark the terminal crossover frequencies.

We observe that in the absence of metal ions, the terminal relaxation of the reference sample is reached at τ_{rel}=25.6ms (with $\tau_{rel}=1/\omega_c$, where the angular frequency ω_c marks the crossover of G' and G''). As discussed in Section III.1, these entangled stars relax their stress by arm retraction. Once the metal ions, Zn(II) or Cu(II), are added, the relaxation process slows-down. For Star250k-Zn-0.75eq., the relaxation time becomes about $\tau_{rel,\ Zn(II)}$=58.8ms. This retardation becomes more significant for star250k-Cu-0.75eq. ($\tau_{rel,\ Cu(II)}$=2500ms, or about 42.5 times slower). Hence, the associated tpy-Cu(II) bis-complexes are significantly more stable and have a longer association time, compared to the tpy-Zn(II) bis-complexes, which have only a weak effect on the viscoelastic properties of the reference stars. This is in line with the reported characteristics of tpy-Cu(II) bis-complexes,[6,43] and with the results obtained on similar systems.[34] However, even in the presence of Cu(II) ions, the metallo-supramolecular networks reach their terminal regime at 40°C, exhibiting $G'(\omega)\sim\omega^2$, $G''(\omega)\sim\omega^1$ at low frequencies. This means that at this temperature, the lifetime of the metal-ligand association is not long enough to prevent the sample from flowing. As further discussed in Section IV.2, the supramolecular

junctions are dynamic and can dissociate and re-associate several times within the experimental frequency window, which leads to a delayed relaxation of the transient network. Therefore, we suggest that the metal-ligand crosslinks act as extra friction points at the arms extremities, and slow-down the stress relaxation (see Section III.2).

B. Single dynamic networks based on Zn(II). We first study the linear viscoelastic behavior of the transient networks with Zn(II), whose content varies from stoichiometric amount, 0.5eq., to excess contents of 0.75eq., 1.0eq. and 1.25eq.. Figure 4 presents the linear rheological behavior of Star250k-Zn at 80°C, 25°C and -20°C and different Zn(II) contents. Upon increasing the amount of metal ions, the relaxation of the networks is gradually delayed. This behavior, which is also observed with the Cu(II) ions, suggests that the probability of a terpyridine ligand to remain associated through the formation of a bis-complex(expectedly) increases with the density of ions.

At a high temperature of 80°C, the delay induced by the supramolecular junctions is less pronounced than compared to 25°C, and the network dynamics resemble those of Star250k-Reference. In this case, the stress relaxation is governed by the disentanglement time of the star arms rather than the sticker lifetime, which becomes much shorter.

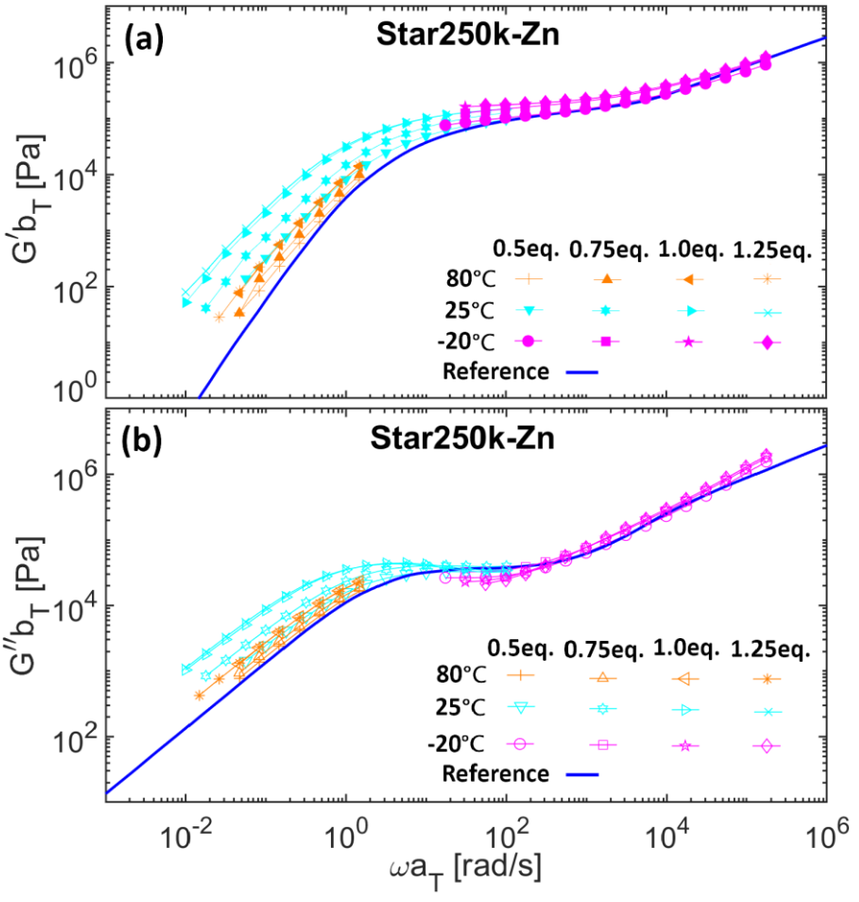

Figure 4. (a) Shifted storage and (b) loss moduli of Star250k-Zn as functions of the shifted frequency at different metal ion content, 0.5eq., 0.75eq., 1.0eq. to 1.25eq. and temperatures of 80°C, 25°C and -20°C. G' is represented by filled symbols and G'' by empty symbols. The data have been shifted to the reference temperature of 25°C, based on the shift factors obtained for the Star250k-Reference sample.

At a low temperature of -20°C, the high-frequency Rouse relaxation is captured, followed by the rubbery plateau. The latter should be approximated by the entanglement rubbery plateau of PnBA, since the density of entanglement segments is much larger than the density of stickers. However, it is observed that for Star250k-Zn-0.5eq., the storage modulus rapidly decreases below G_N^0. This is attributed to the presence of a large fraction of dangling ends, which do not participate to network formation and relax as the star arms of the reference sample. In such a case, the dangling ends mostly include unassociated arms. Indeed, as discussed in ref. [35], the weight fraction of metal ions is so low

(i.e., 0.003-0.008 wt%) that we cannot exclude the possibility that some terpyridine ligands do not find a free ion in their surroundings to form a complex. In the presence of an excess amount of metal ions, the fraction of dangling ends decreases. This effect can be inferred by the more pronounced and nearly unchanged plateau modulus of Star250k-Zn-1.0eq. and Star250k-Zn-1.25eq., which suggests that the supramolecular network is at its maximum level of crosslinking at 1.0eq.Zn(II). It must be noted that phase separation of the complexes was not observed for these systems, based on SAXS measurements.

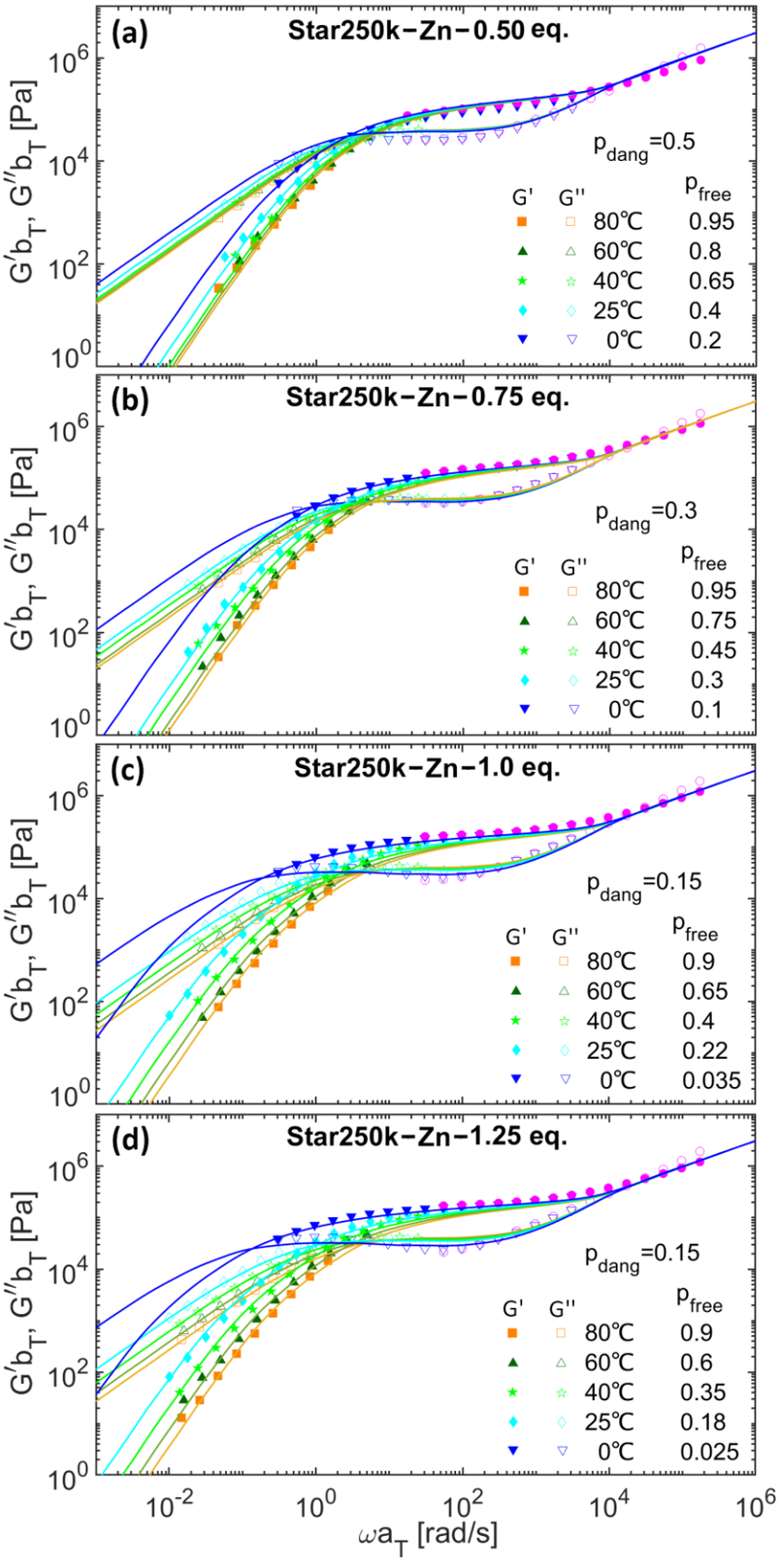

Figure 5. Linear viscoelastic master curves: Comparison between experimental data (symbols) of Star250k-Zn with increasing ion content and model predictions (continuous curves) for (a) Star250k-Zn-0.5eq. (b) Star250k-Zn-0.75eq. (c)

Star250k-Zn-1.0eq. and (d) Star250k-Zn-1.25eq.. G' is represented by filled symbols and G'' by empty symbols. The data have been shifted to the reference temperature of 25°C, based on the shift factors obtained for the Star250k-Reference sample. The theoretical curves were determined by respectively fixing a certain proportion of dangling ends at different ion content and varying the value of the parameter p_{free} at each temperature.

In order to quantify the influence of the ion content, the linear viscoelastic master curves were modeled by means of the modified TMA model (continuous curves) at different temperatures from 0°C to 80°C. To account for the influence of temperature on the segmental dynamics, the data were horizontally shifted with the shift factors of the Star250k-Reference sample. In such a way, the remaining difference in relaxation times observed by varying the temperature is only due to the influence of temperature on sticker dynamics. Results are presented in Figure 5. It can be observed that the retardation of the relaxation process is enhanced with decreasing temperature, which can be attributed to the enhanced stability of the metal-ligand associations.

The model captures the linear viscoelastic spectra well (see Equation 8) by using two fit parameters, namely the fraction of dangling ends, p_{dang}, and the average time during which the sticker is free, p_{free}. The best-fit values are shown in Figure 6. The fraction p_{dang} decreases with increasing metal ion content as shown in Figure 6.a. Indeed, 50%, 30%, 15% and 15% of dangling ends have been considered to obtain a good description of the rheological data of the transient networks containing 0.5eq., 0.75eq., 1.0eq. and 1.25eq. of Zn(II), respectively. On the other hand, Figure 6.b depicts the dependence of p_{free} on ion content at each temperature. While the influence of temperature on the association probability is further discussed in Section IV.3, several observations can already be made. From 0.5eq. to 1.25eq., the parameter p_{free} is slightly dependent on ion content at high temperatures (60°C and 80°C). This is consistent with the fact that at these temperatures the stability of tpy-Zn(II) bis-complexes is relatively weak, and thus the stickers do not cause significant delay (due to extra friction) to the motion of the star arms. Consequently, the relaxation process of these transient networks is mainly governed by the disentanglement dynamics, which sets the minimum time a star arm needs to relax. On the other hand,

at lower temperatures, i.e., 25°C or 0°C, p_{free} is becoming much smaller and exhibits a stronger dependence on ion content. Here, the sticker lifetime is much longer and the arm relaxation process is largely influenced by the dynamics of the supramolecular junctions.

The fact that the probability p_{free} decreases with increasing the content of metal ions is attributed to the evolution of the fraction of dangling ends. Indeed, at low metal ion content the relaxation of the transient network speeds-up due to the presence of free ends, which promote the dissociation of the bis-complexes via ligand exchange mechanism.[17,35,44] Adding an excess of ions reduces the proportion of free ends, and consequently the ligand exchange process, leading to slower star arm relaxation. This result also suggests that the presence of mono-complexes is not favored in our systems in the range of ion content considered since it would have led to an increase of dangling ends with increasing the ion content, which is not observed. Probably, a much larger amount of ions should be used to observe this effect.

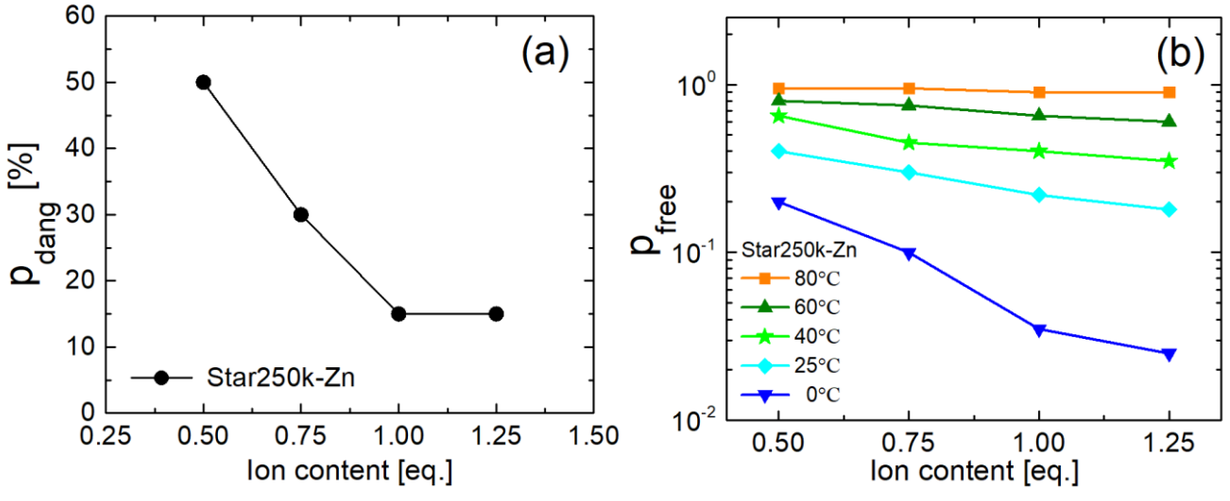

Figure 6. The model parameters referring to the master curves of Figure 5: (a) the proportion of dangling ends p_{dang} and (b) fraction of time when ends are dissociated p_{free} for Star250k-Zn as functions of metal ion content at 0°C, 25°C, 40°C, 60°C and 80 °C.

In order to validate the possible presence of dangling ends even above the stoichiometric amount of

Journal of Rheology

ions, the transient networks were analyzed by FTIR absorption spectroscopy. By comparing the FTIR absorption spectrum of the reference sample (Star250k-tpy4) to the one of a pure, unfunctionalized linear PnBA polymer (M_w = 26kg/mol), we can assign the absorption bands corresponding to the vibrations of the terpyridine groups.[45,46] As shown in Figure 7.a, the latter are located in the wavenumber range of 1560-1610cm^{-1}. Figure 7.b, shows that once the Zn(II) ions are added, a new band appears at 1614cm^{-1}, i.e., just after the absorption bands corresponding to the terpyridine groups. It reflects the complexation of the terpyridine with metal ions. With increasing ion content, the intensity of the new absorption band gradually increases, while the opposite effect is observed for the absorption bands at 1564cm^{-1} and 1583cm^{-1}, which slowly decrease, indicating that the proportion of the non-coordinated ligands decreases and the complexation progressively yields to completion.

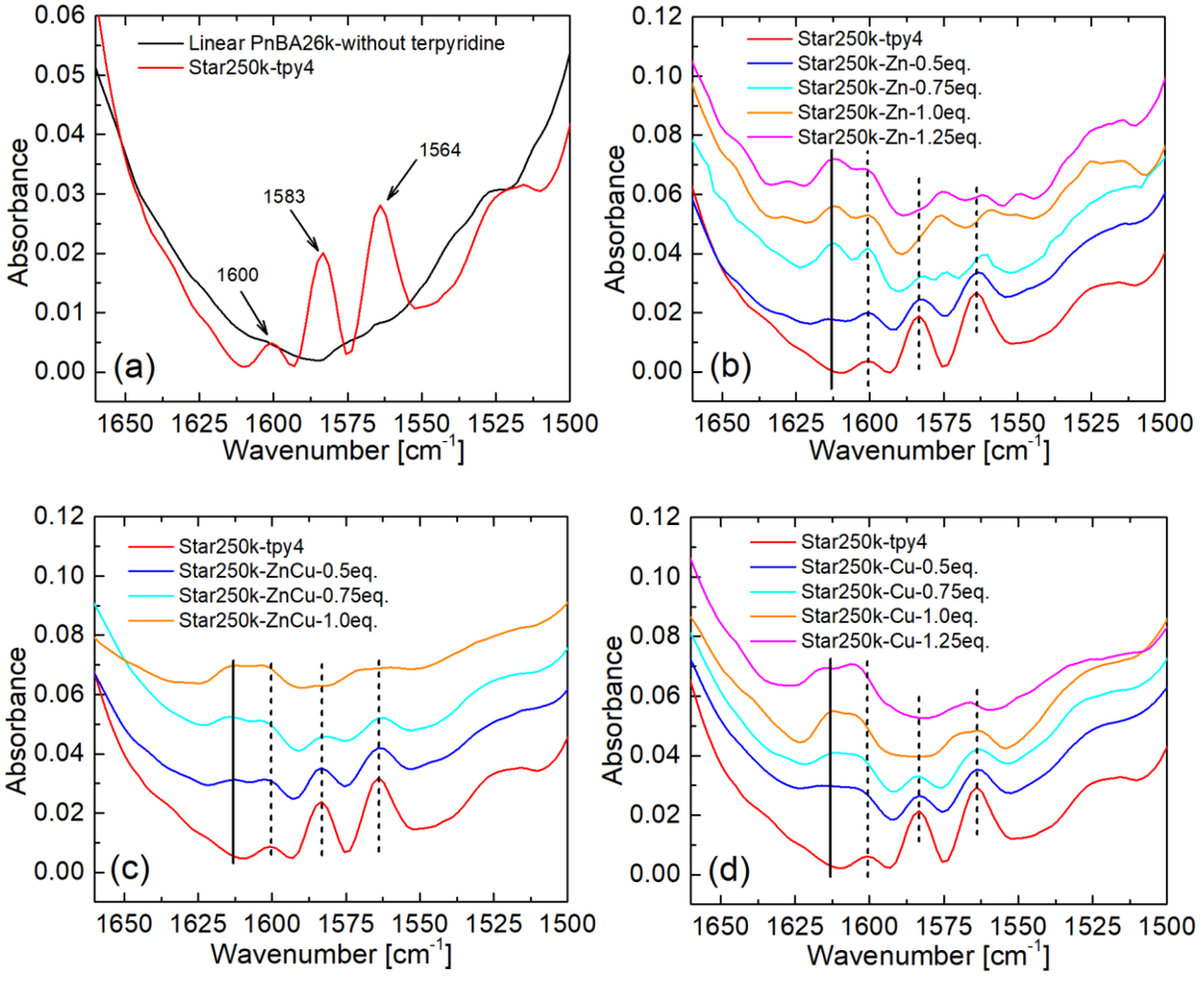

Figure 7. FTIR spectra of (a) Star250k-tpy4 and linear PnBA26k without terpyridine (b) Star250k-Zn (c) Star250k-ZnCu and (d) Star250k-Cu at room temperature as the ratio of metal ion to ligand increases (spectra are shifted vertically for comparison). From bottom to top in plots (b), (c) and (d), the curves denote reference sample, 0.5eq., 0.75eq., 1.0eq. and 1.25eq.(for d).

Interestingly, even at 0.75eq. of metal ions, i.e., above the stoichiometric amount of Zn(II), the absorption peaks at 1564cm^{-1} and 1583cm^{-1} still exist, confirming the presence of non-coordinated ligand in the system, consistently with the assumption of the presence of dangling ends.

C. Single dynamic networks in the presence of Cu(II). As shown in Figure 8, adding Cu(II) to the telechelic star polymers yields the formation of a transient network which is more stable compared to Zn(II). In Particular, at 80°C, the influence of the ions on network dynamics is larger (for Cu(II)) with ion content of at least 0.75eq.. Therefore, the relaxation of the transient network is not governed by the entanglements anymore, as in the case of Zn(II). Similarly to Zn(II)-containing networks, increasing the metal ion density slows-down the relaxation process, due to the decreasing fraction of dangling ends. Indeed, at lower temperatures (-20°C and 25°C) it is observed that samples Star250k-Cu-0.5eq. and Star250k-Cu-0.75eq. partially relax at intermediate frequencies around 10 rad/s, which coincides with the relaxation of the reference sample. Furthermore, the networks exhibit a broad and slow relaxation at 25°C, which cannot be explained if we only consider one single process governed by the sticker dynamics. On the other hand, there is an extended rubbery plateau with 1.0eq. or 1.25eq. Cu(II), while the early relaxation process becomes less pronounced. The presence of dangling ends is also confirmed by the FTIR spectra (see Figure 7.d).

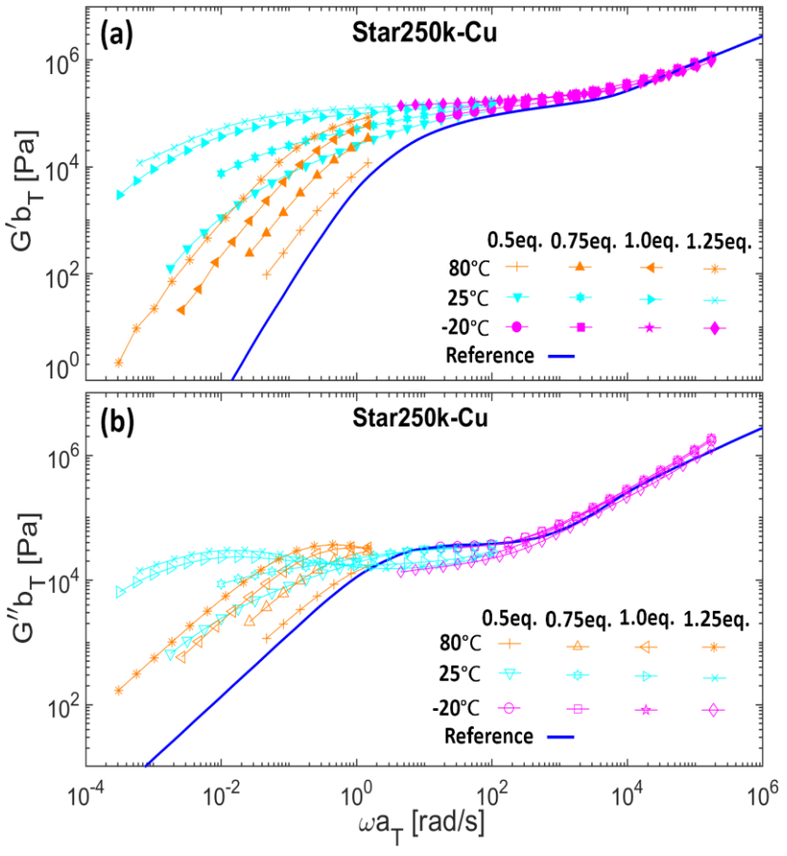

Figure 8. (a) Storage modulus and (b) loss modulus of Star250k-Cu with increasing ion content from 0.5eq. to 1.25eq. at 80°C, 25°C and -20°C. G' is represented by filled symbols and G'' by empty symbols. The data have been shifted to the reference temperature of 25°C, based on the shift factors obtained for Star250k-Reference sample.

We now apply our TMA model to describe the experimental data. Results are depicted in Figure 9, which compares the experimental data with model predictions for Star250k with 0.5eq., 0.75eq., 1.0eq. and 1.25eq. Cu(II). In order to experimentally reach the terminal *G', G''* cross-over frequencies, creep measurements were performed and converted into the dynamic moduli. The fraction of dangling ends is found to be 60%, 35%, 25% and 20% respectively. We note that accounting for these dangling ends and the delay in the fluctuation time of the associating stars yields a good agreement for most of the experimental data. The values of the two fit parameters, p_{dang} and p_{free}, are denoted in Figure 9 and their dependence on ion content and temperature is presented in Figure 10. Both parameters exhibit a trend similar to that observed with Zn(II). However, the value of p_{free} has a stronger dependence on ion

content and especially at higher temperatures. Furthermore, its value remains well below 1, which corresponds to the state where the star relaxation is fully governed by the disentanglement process.

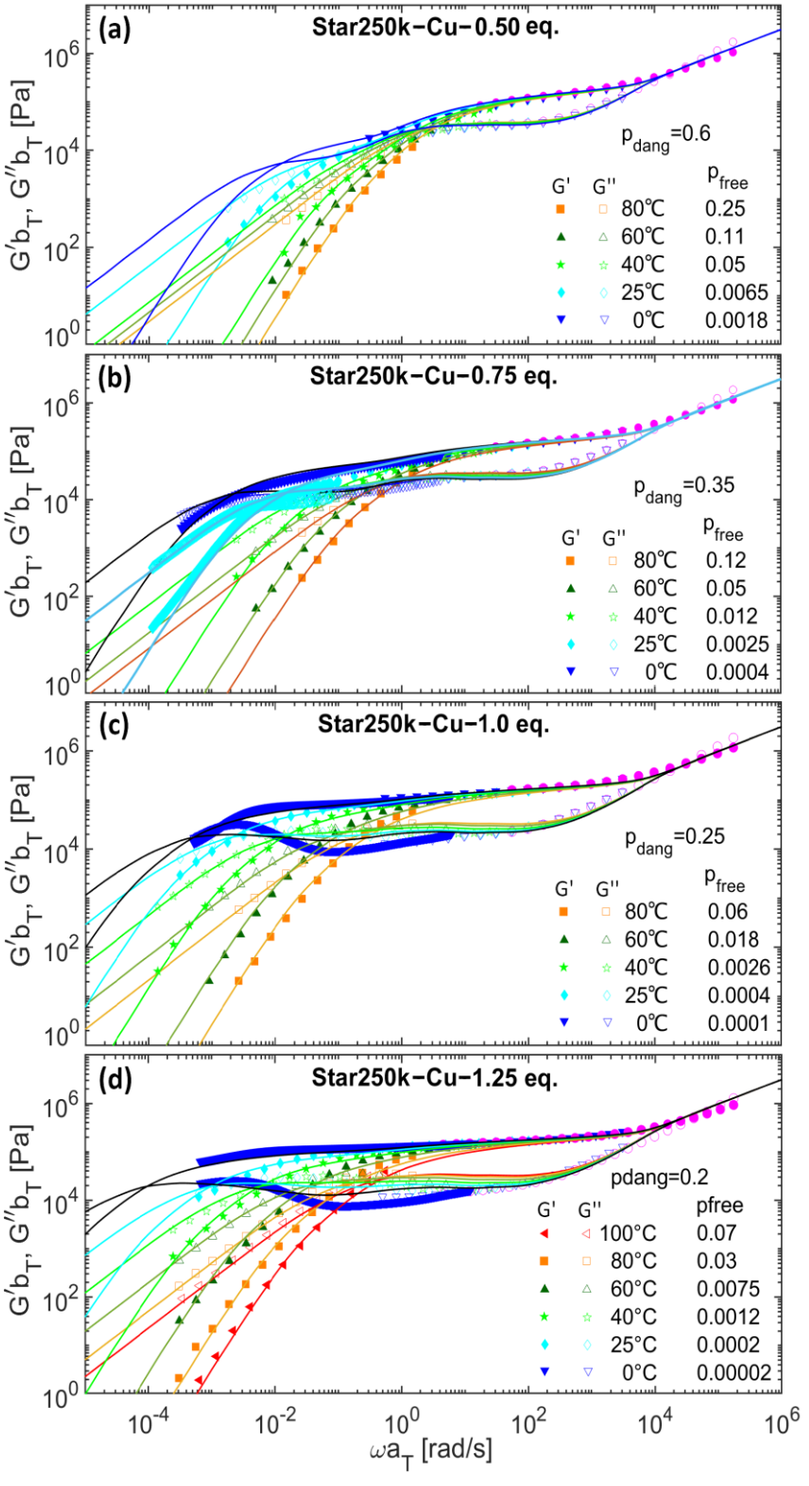

Figure 9. Comparison between experimental data (symbols) of Star250k-Cu with increasing ion content and model

predictions (continuous curves). Shown are linear viscoelastic master curves for (a) Star250k-Cu-0.5eq. (b) Star250k-Cu-0.75eq. (c) Star250k-Cu-1.0eq. and (d) Star250k-Cu-1.25eq.. The experimental dynamic moduli for samples with 0.75eq.Cu at 0°C and 25°C as well as sample with 1.0eq.Cu and 1.25eq.Cu at 0°C have been extended by means of creep measurements; the respective data are shown as different symbols at low frequencies (see text). The experimental data have been shifted to the reference temperature of 25°C, based on the shift factors obtained for Star250k-Reference sample. The theoretical curves were determined by respectively fixing a certain fraction of dangling ends at different ion content and varying p_{free} value at each temperature.

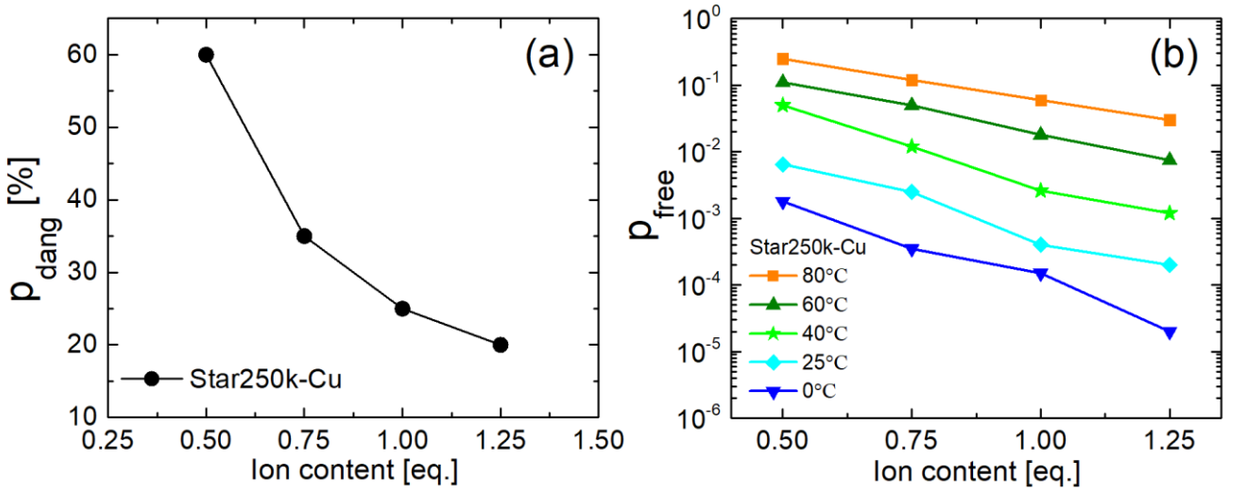

Figure 10. Model parameters referring to the master curves of Figure 9, (a) the proportion of dangling ends p_{dang} and (b) fraction of time when ends are dissociated p_{free} for Star250k-Cu as functions of ion content at 0°C, 25°C, 40°C, 60°C and 80 °C.

While the simple approach proposed in Equation 8 seems to successfully account for the influence of the sticker dynamics, one should note however that in Figure 9, the discrepancy between the model predictions and the experimental data increases at lower temperatures. In particular, with samples Star250k-Cu-1.0eq. and Star250k-Cu-1.25eq. at 0 °C, we observe experimentally two relaxation peaks in the loss moduli of the samples, which are absent in the model.

This discrepancy is attributed to the fact that the influence of the stickers is taken into account in the model as an *average* effect on the relaxation time and therefore is only valid at long times, when a sticker has had the chance to dissociate and re-associate multiple times. Since at low temperatures the

re-association lifetime of the stickers is much longer, this assumption is not valid anymore and a more refined model is needed in order to account for the inability for an associated arm to relax at times shorter than the lifetime of the sticker, $t < \tau_{sticker}$. To do so, we apply an approach similar to ref. [33] and consider an average lifetime $\tau_{sticker.}$, which is used to build the corresponding statistical distribution of sticker lifetimes (τ_i, ν_i), based on the assumption that the probability of a sticker to dissociate during a short time step Δt is $\exp\left(-\frac{\Delta t}{\tau_{sticker}}\right)$. This distribution of lifetimes is then used to determine the survival probability of a segment x along the star arm. More precisely, we consider that the probability for a sticker with an association lifetime τ_i, to remain associated at time t is equal to $exp\left(\frac{-t}{\tau_i}\right)$. Consequently, a fraction $exp\left(\frac{-t}{\tau_i}\right)$ of those specific stickers should be considered as unable to relax at time t. The survival probability of a molecular segment x along an arm attached to the network via a sticker of lifetime τ_i is thus approximated as:

$$p_{fluc}(x,t,\tau_i) = \left[exp\left(\frac{-t}{\tau_i}\right) + \left(1 - exp\left(\frac{-t}{\tau_i}\right)\right) p\left(\frac{-p_{free}\, t}{\tau_{fluc}(x)}\right)\right] \quad (9)$$

Equation 9 can be generalized, by accounting for both the dangling ends and the distribution of sticker lifetimes, τ_i:

$$p_{fluc}(x,t) = p_{dang}\, exp\left(\frac{-t}{\tau_{fluc}(x)}\right) + (1 - p_{dang})\, \sum_i \nu_i\, p_{fluc}(x,t,\tau_i). \quad (10)$$

The results obtained by using Equations 9 and 10 are shown in Figure 11. The values of parameters p_{dang} and p_{free} are in very good agreement to those used in Figures 9 and 10, while the association time $\tau_{sticker}$ has been obtained by best-fitting. It is observed that accounting for the short-time limitation provides a better description of the data, however at the expense of introducing a new parameter, $\tau_{sticker}$. The value of this parameter is further discussed in Section IV.3.

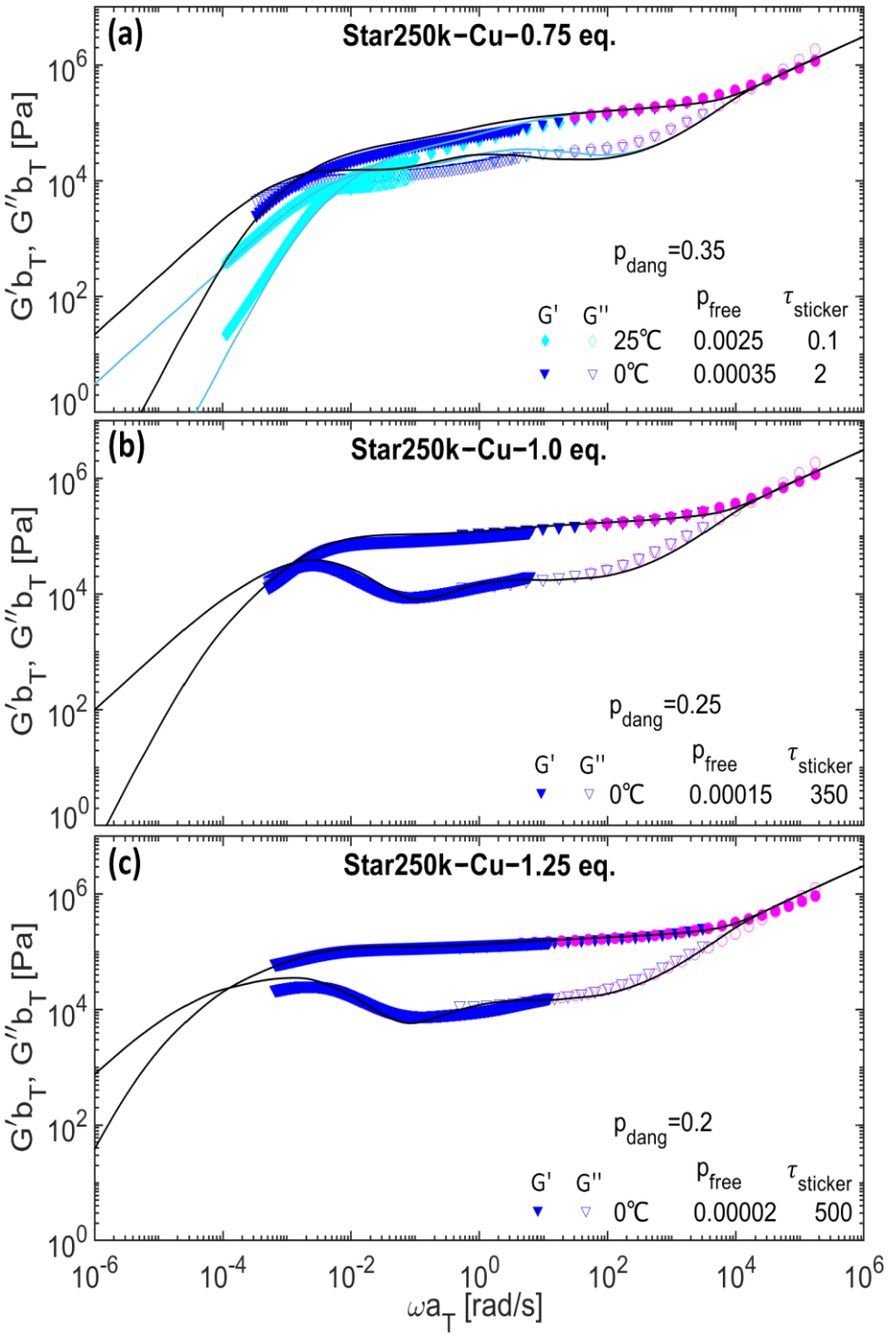

Figure 11. Comparison between linear viscoelastic experimental data (symbols) and model predictions (continuous curves) obtained by accounting for the lifetime of the stickers (Equation 9), for (a) Star250k-Cu-0.75eq. (b) Star250k-Cu-1.0eq. and (c) Star250k-Cu-1.25eq.. The dynamic moduli data for samples with 0.75eq.Cu at 0°C and 25°C as well as sample with 1.0eq.Cu and 1.25eq.Cu at 0°C have been extended by means of creep measurements. The data have been shifted to the reference temperature of 25°C, based on the shift factors obtained for the reference sample. The theoretical curves were determined based on the parameters p_{dang} and p_{free} used in Figures 9 and 10. The lifetime of the stickers, $\tau_{sticker}$, was fixed to 0.1s at 25 °C for sample Star250k-Cu-0.75eq.. At 0 °C, $\tau_{sticker}$ was fixed to 2s, 350s and 500s for samples containing

0.75eq.Cu, 1.0eq.Cu and 1.25eq.Cu, respectively.

IV.2. Double dynamics networks

In Section IV.1., it was shown that the dynamics of the transient networks strongly depend on the ion type, the Zn(II) complexes being more labile than the Cu(II) complexes. We now extend our approach to double metal ion networks by mixing Zn(II) and Cu(II), with the objective to investigate the competition between the two ions in the formation of complexes and their influence on the dynamics.

The influence of mixing the ions at different amounts (0.5eq., 0.75eq. and 1.0eq. of ions per equivalent of terpyridine group) on the linear viscoelastic response of double dynamics networks is depicted in Figure 12, at a temperature of 60°C. Interestingly, blending two ions of different natures leads to an average cooperative behavior of the stickers' dynamics, characterized by a single relaxation peak, rather than two relaxation peaks corresponding to the respective sticker lifetimes. This result suggests that the sticker associates and dissociates many times before the corresponding arm is fully relaxed. Similar behavior has already been observed with PEG hydrogel networks containing kinetically distinct reversible covalent crosslinks. The viscoelastic response of these systems was found to be independent of the molecular weight of the building blocks.[47] Similarly, Chen et al. showed that unentangled hydrogels crosslinked by one type of sticker but in two different states, i.e. protonated and deprotonated states characterized by two different lifetimes, also exhibit a single intermediate relaxation time.[48] In contrast, Grindy et al. found that the signature of each metal-ligand junction was preserved in the viscoelastic spectra of unentangled PEG hydrogels with two different metal-histidine crosslinks.[25] Thus, these different works show that the viscoelastic response of a network containing two different stickers can strongly vary, depending on the relative dynamics of the building blocks and of the reversible bonds. In our system, each arm reaches its terminal regime only after being involved

in both fast and slow bis-complexes multiple times and, consequently, their corresponding final relaxation time is averaged. We attribute this effect to the fact that the star molecules are entangled, and therefore have long relaxation times. Indeed, since the average time during which a sticker remains free is relatively short (see Section IV.3), it does not allow a free arm to fully disentangle before being again involved in a bis-complex. Therefore, the different behavior observed here compared to ref. [25], which deals with unentangled gels, reflects the different balance between supramolecular dynamics and relaxation of the building blocks.

This scenario is further supported by the fact that for most of the present data, the supramolecular dynamics lead to an overall delay of arm relaxation. The latter is described by a single parameter, p_{free} in our model (Equation 8), i.e., assuming that at any time t we can consider that all stickers are free to move during an average time $p_{free}\, t$. This would not have been the case if a star arm would have been able to fully relax as soon as the sticker dissociates, which would have led to a relaxation described by a single Maxwell element with a characteristic relaxation time equal to $\tau_{sticker}$.

In Figure 12, it is also observed that the viscoelastic behavior of the double dynamics networks lies between the responses of the single dynamic networks, and gradually shifts from a behavior close to the weaker network containing 0.5eq.Zn(II)) to that of the stronger one containing 1.0eq.Cu(II)) ions. This can be rationalized by considering that at stoichiometric amount, the double dynamics network relaxes relatively fast due to the presence of a large amount of dangling ends. Exchange dynamics are promoted and take place at the rhythm of the faster sticker motion. Upon increasing ion content, a reduced influence of dangling ends is expected, and the stars relax slower. This can be observed in the FTIR spectra in Figure 7.c, which shows that the double dynamics network has a pattern similar to that of the single metal ion networks. Moreover, the absorption bands between1600cm^{-1} and 1620cm^{-1} of Star250k-ZnCu is much closer to that of Star250-Cu than the one of Star250-Zn network, especially

with an excess of metal ions of 0.75eq. and 1.0eq. This suggests that the Cu(II) has a dominant effect on the complex formation when the ions are added in excess.

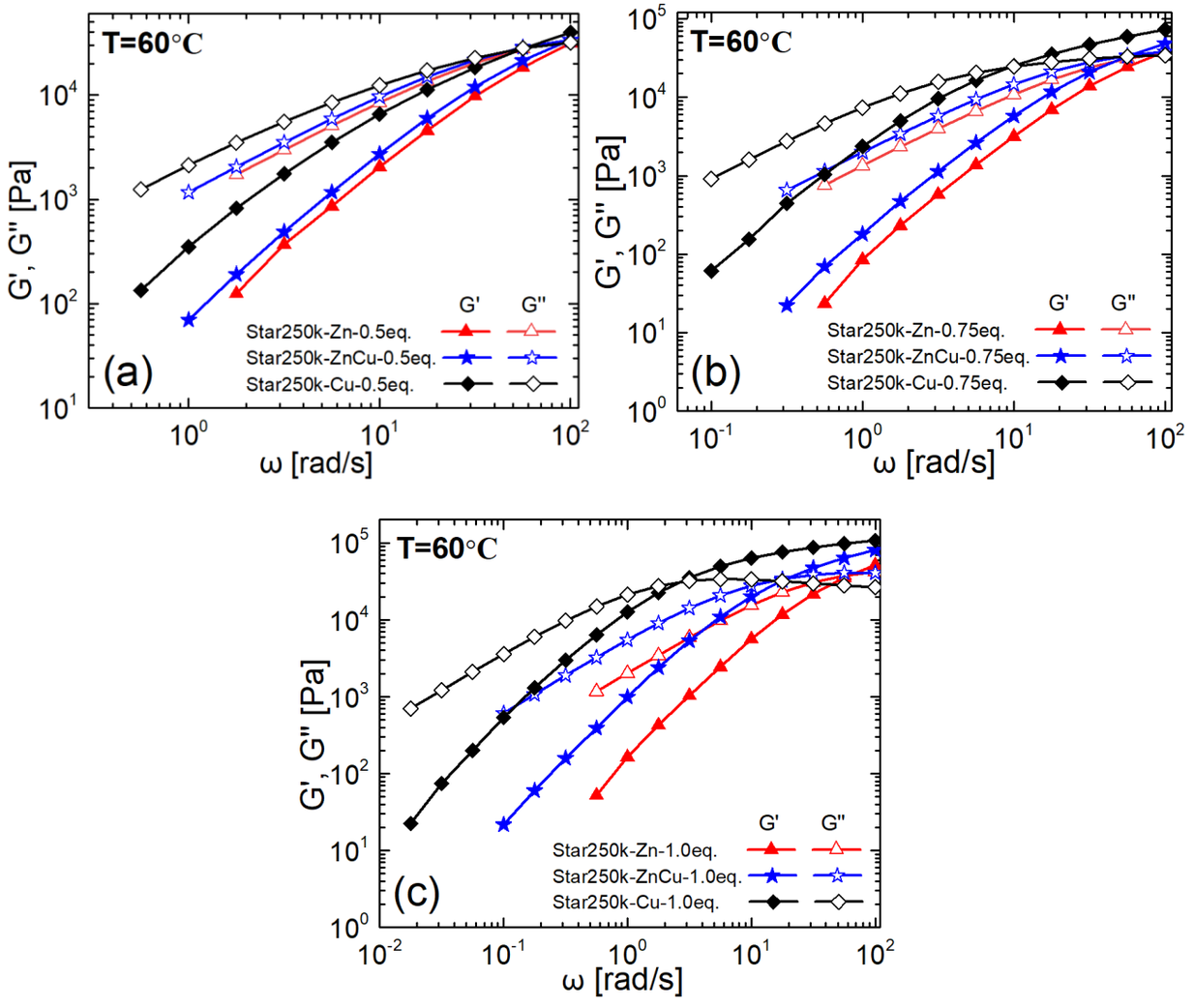

Figure 12. Comparison of the frequency-dependent storage modulus and loss modulus between Star250k single dynamic network and double dynamics networks with increasing ion content from (a) 0.5eq., (b) 0.75eq. to (c) 1.0eq. at 60°C. G' is represented by filled symbols and G'' by empty symbols.

The dominant effect of Cu(II) is further rationalized by considering the mass balance and equilibrium constants (K_1 for mono-complexes and K_2 for bis-complexes) for terpyridine coordinated with Zn(II) and Cu(II). The latter values are taken from the literature.[43,46,49,50] It should be noted that only two kinds of metal-ligand complexes, either mono-complexes or bis-complexes, can be formed once

divalent metal ions are added, such as Zn(II) and Cu(II).[6,46,51] As illustrated in Figure 13.a, these constants and the ratio of metal to ligand determine the fraction of free ligands, free metal ions, bis-complexes and mono-complexes present in the double dynamics networks. As shown in Figure 13.b, assuming that the initial molar amount of terpyridine is held constant at $4x10^{-6}$mol in total (250mg of Star250k polymer), while the amount of each metal ions varies from $0.5x10^{-6}$mol (0.25eq.) to $2.5x10^{-6}$mol (1.25eq.). It becomes evident that adding ions in excess compared to their stoichiometric amount promotes the formation of bis-complexes involving Cu(II), instead of Zn(II).

However, this result must be considered with care since in this simple calculation the protonation of the ligand and the reaction of free metal ions with solvent molecules and anions are not taken into account. Also, the variation of different species is determined in solution state (K_1 and K_2 values have been obtained in water). Hence, there may be some differences with respect to the melt state of our samples. Nevertheless, this simple analysis can be qualitatively used to describe the evolution of the fractions of the different species involved in the formation of complexes. Herein, results suggest that the proportion of Cu(II) ions involved in the network is larger than the proportion of Zn(II) with samples containing an excess of ions. This could explain why the viscoelastic curves are gradually shifting towards the single dynamic networks with Cu(II).

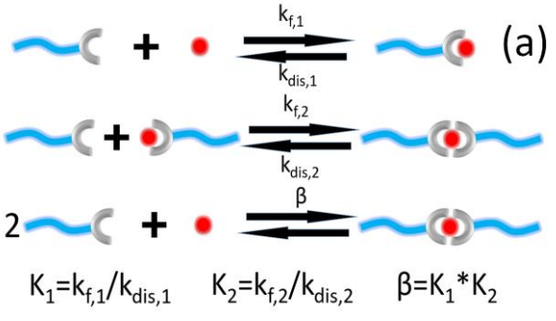

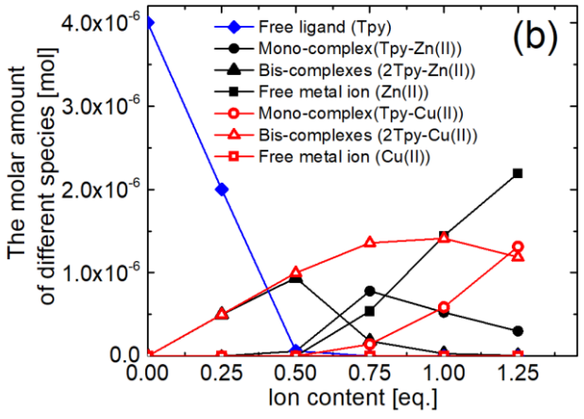

Figure 13. (a) Schematic representations of association/dissociation equilibrium for metal-ligand bond. K_1 and K_2 are the equilibrium constants for mono- and bis-complexes, respectively. ($k_{f,1}$ and $k_{dis,1}$ as well as $k_{f,2}$ and $k_{dis,2}$ are the formation and dissociation constants for mono-complex and bis-complexes, respectively). (b) The equilibrium molar amount of the different species involved: ligand L, metal M, mono-complex ML and bis-complexes ML_2, are calculated and plotted as a function of the ratio of metal ion to ligand (The equivalent amount on the horizontal axis means equivalent of each metal ion, e.g., 1.0eq. means blending 1.0eq.Cu(II) and 1.0eq.Zn(II)) based on mass balance using equilibrium constants K_1 and K_2 from literature for double dynamics networks containing same equivalent of Zn(II)($K_1=10^6$ M^{-1} and $K_2=10^{5.2}$ M^{-1}) and Cu(II)($K_1=10^{12.29}$ M^{-1} and $K_2=10^{6.82}$ M^{-1}).

In Figure 13.b, we see that an excess of metal ions promotes the formation of mono-complexes, which are accounted for as free dangling arms in our model. However, from our rheological modeling we cannot see this overall increase of dangling ends at large ion content. In addition to the qualitative character of Figure 13.b, this discrepancy is attributed to the fact that our samples are in bulk state and contain a very low weight fraction of ions, leading to a proportion of non-active ions and consequently, to an effective ion content lower than that indicated on the plot. For the same reason, Figure 13.b indicates that there are no free ligands at stoichiometric amount of ions, while the FTIR data clearly show that they still exist (Figure 7.c). By taking into account the presence of dangling ends, the comparisons between theoretical and experimental linear viscoelastic curves of the double dynamics networks are shown in Figure 14.

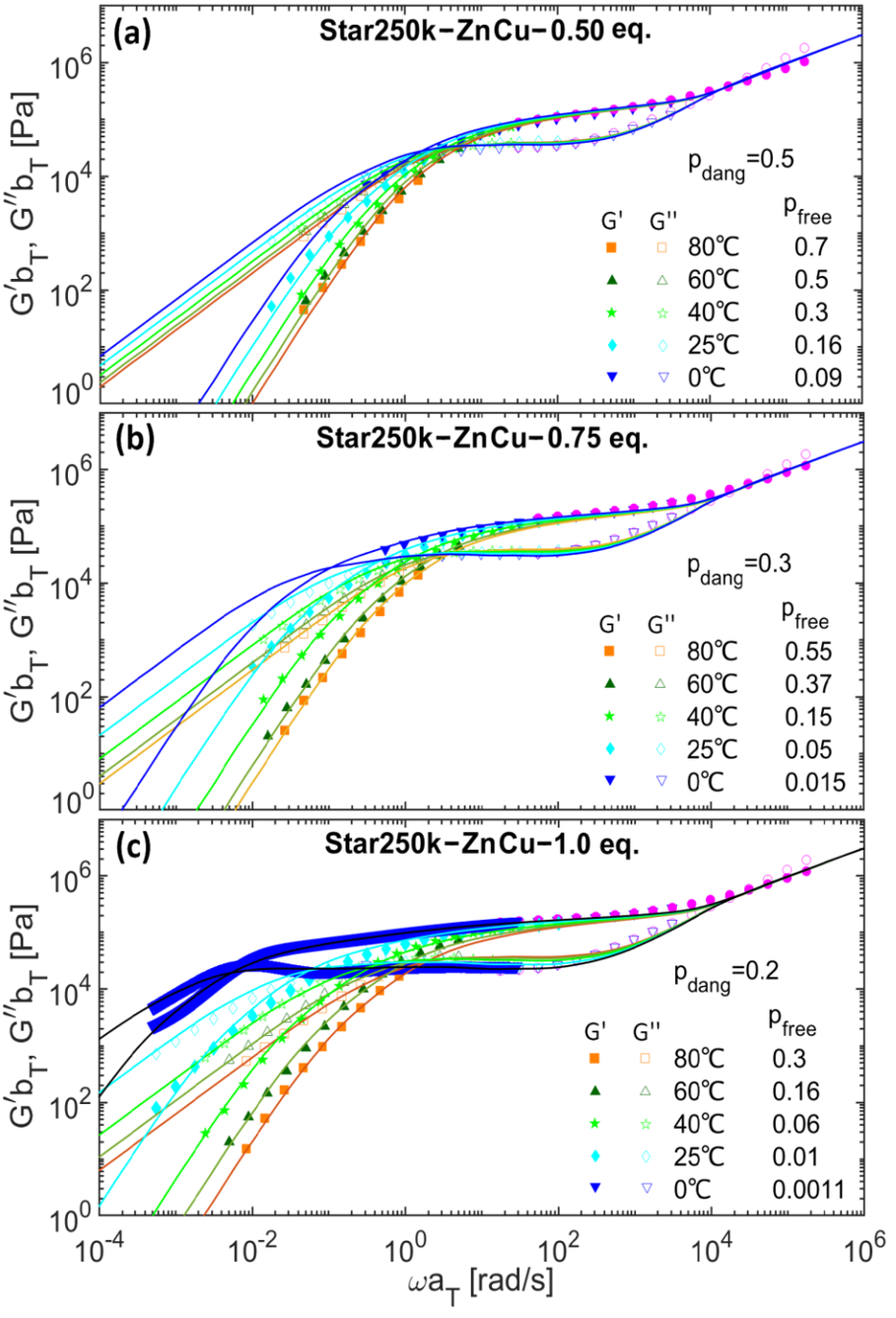

Figure 14. Comparison between experimental data (symbols) of Star250k-ZnCu with increasing ion content and model predictions (continuous curves) of linear viscoelastic master curves for (a) Star250k-ZnCu-0.5eq. (b) Star250k-ZnCu-0.75eq. and (c) Star250k-Cu-1.0eq.. The dynamic modulus data for sample with 1.0eq.Zn and 1.0eq.Cu at 0°C were extended with creep measurements. The data have been shifted to the reference temperature of 25°C, based on the shift factors obtained for Star250k-Reference sample. The theoretical curves were determined by fixing a certain proportion of dangling ends at different ion content and varying p_{free} value at each temperature.

A satisfactory agreement is found based on the model parameters shown in Figure 15. While the trend is similar to the case of single dynamic networks (Figures 6, 10), here the values of p_{free} exhibit a stronger dependence on ion content, compared to star250k-Zn counterpart. This is attributed to the increasing fraction of tpy-Cu(II) complexes with respect to tpy-Zn(II) complexes in the blends.

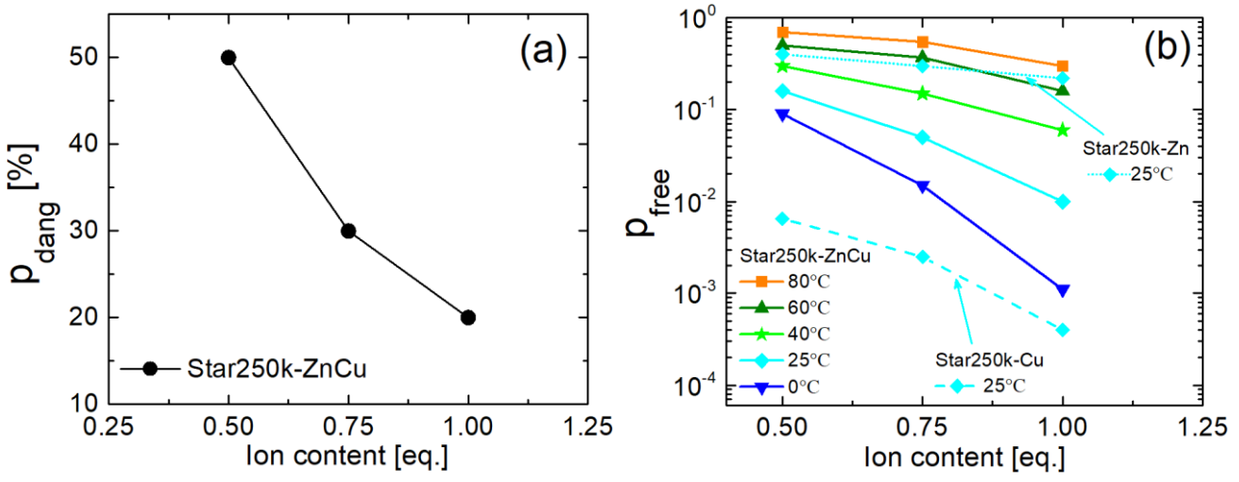

Figure 15. The model parameters referring to the master curves of Figure 14: (a) the proportion of dangling ends p_{dang} and (b) the fraction of time when stickers are unassociated p_{free} for Star250k-ZnCu as function of ion content at 0°C, 25°C, 40°C, 60°C and 80°C. The results obtained at 25°C for Star250k-Zn and Star250k-Cu are also shown for comparison.

IV.3. Influence of temperature.

As discussed in the previous sections, the dynamics of the metallo-supramolecular networks is primarily controlled by the metal-ligand coordination which itself is strongly dependent on the temperature. Since our results indicate that these metallo-supramolecular networks reach their maximum level of crosslinking at 1.0eq. of metal ions, where most of the arms are being involved in the network, we focus on the dynamics of both single and double dynamics networks at this ion content to investigate the influence of the temperature. The linear rheological behavior of the transient networks at 80°C, 25°C, 0°C and -20°C is presented in Figure 16.

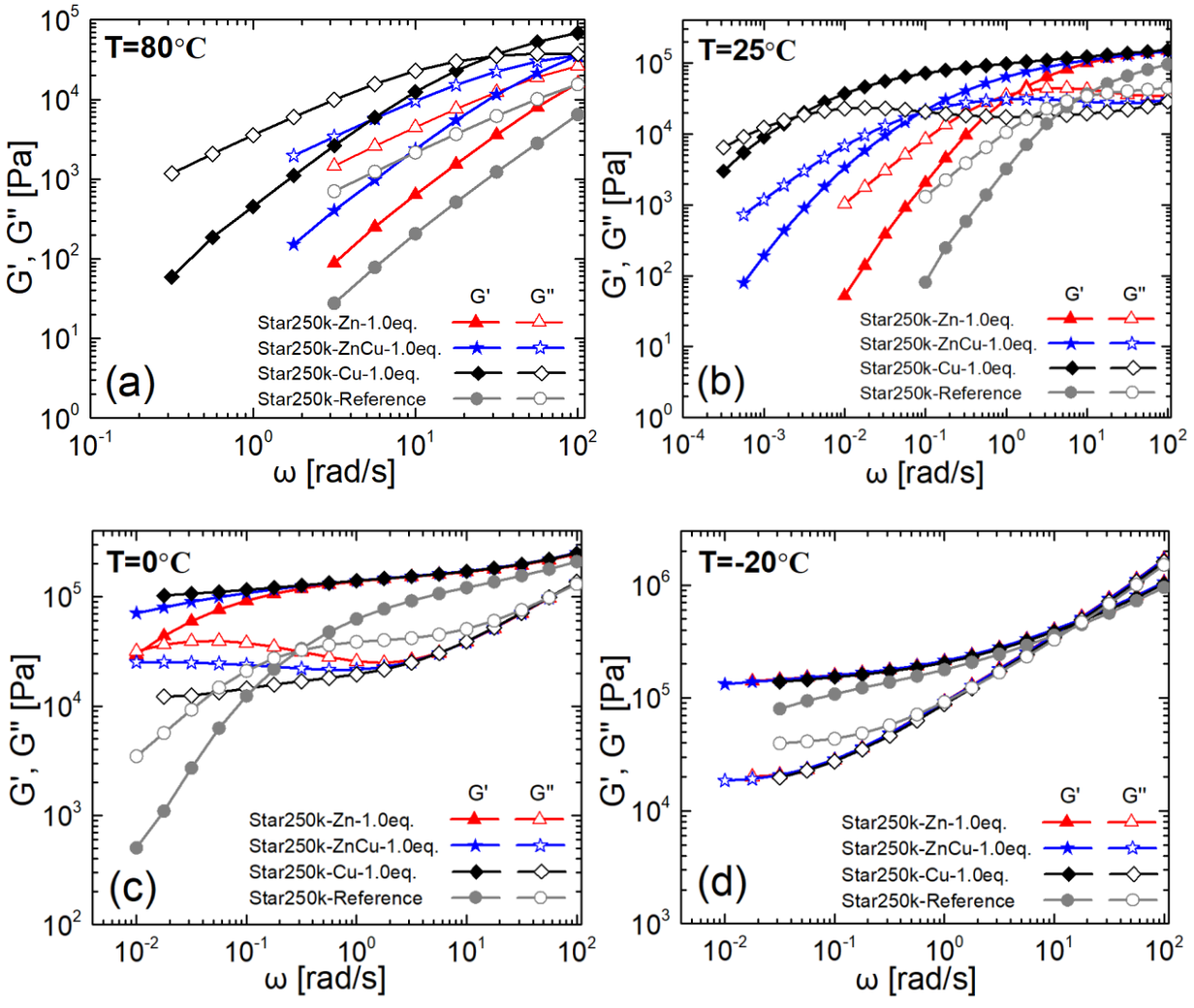

Figure 16. Frequency-dependent storage and loss moduli of Star250k-Reference, Star250k-Zn-1.0eq., Star250k-ZnCu-1.0eq. as well as Star250k-Cu-1.0eq. at (a) 80°C, (b)25°C, (c)0°C and (d)-20°C. G' is represented by filled symbols and G'' by empty symbols.

At -20°C, both the single and double dynamics networks exhibit viscoelastic solid response with the dynamics of the stickers being frozen in the experimental frequency window. We observe a similar high-frequency response at 0°C. However, the metal-ligand dynamics become visible and starts to influence the dynamics of the corresponding network. In particular, the sticker dynamics are probed on the loss modulus at a frequency of about 4rad/s in case of the transient network containing Zn(II) ions. This frequency is much larger than the terminal cross-over frequency and can be assigned to the onset of the dissociation/association dynamics of the Zn(II)-terpyridine transient crosslinks at 0°C. At

higher temperatures, it is expected that the association/dissociation dynamics are accelerated and therefore become active at times even shorter than 0.25s. This is consistent with the conclusion of Section IV.1, according to which the dynamics of the transient bonds are much faster than the cross-over relaxation time τ_{rel}. Depending on the metal ions, the data are strongly influenced by the sticker dynamics at 25°C with the terminal cross-over frequency varying up to four orders of magnitude. At 80°C, the metal-ligand bonds are relatively weak and the terminal relaxation of all samples is dominated by the chain disentanglement dynamics.

Based on results of Figure 16, it can be concluded that a temperature of 0°C is the temperature where the stickers are slow enough to probe the transition from a frozen to a dynamic transient network. This is consistent with the discussion in Section IV.1, where at this temperature the model assumption, that the stickers have an average effect on retarding the network relaxation, does not hold anymore. Therefore, we had to consider that an associated arm cannot relax faster than the lifetime of the sticker (see Equations 9 and 10).

Influence of temperature on the model parameters.

As already mentioned, since the master curves were built at a reference temperature of 25°C based on shift factors obtained from Star250k reference sample, the influence of temperature on the segmental dynamics is already taken into account and the data only reflect the influence of temperature on the metal-ligand transient crosslinks. Therefore, our model parameter p_{free}, which represents the fraction of time when a sticker is free, is related to the nature and the dynamics of the metal-ligand association. This fraction depends on both the average time when an associated sticker remains associated, $\tau_{sticker}$, and the average time when a free sticker stays free, τ_{free} and can be approximated as[33]:

$$p_{free} = \frac{\tau_{free}}{\tau_{free}+\tau_{sticker}}. \quad (11)$$

This single parameter is sufficient to describe the viscoelastic data at angular frequency of $\omega << 1/\tau_{sticker}$. Figure 17 illustrates the dependence of p_{free} as a function of the inverse temperature in a semi-log plot, at 0.5eq., 0.75eq., 1.0eq. and 1.25eq. for both single and double metal ion networks. With decreasing temperature, p_{free} gradually decreases, which is attributed to the higher stability of the bis-complexes at low temperatures and consequently their longer association time. It is also observed that all sets of data collapse into a line, which indicates an Arrhenius dependence of this parameter on temperature. The value of p_{free} for double dynamics networks lies between the corresponding single dynamic networks. With increasing ion content, p_{free} gradually shifts towards the values of Cu(II). This is consistent with the linear rheological behavior of single and double dynamics networks. As discussed above, this is due to that fact that a larger fraction of the Cu(II) ions is involved in the metal-ligand complexes when the ion content increases.

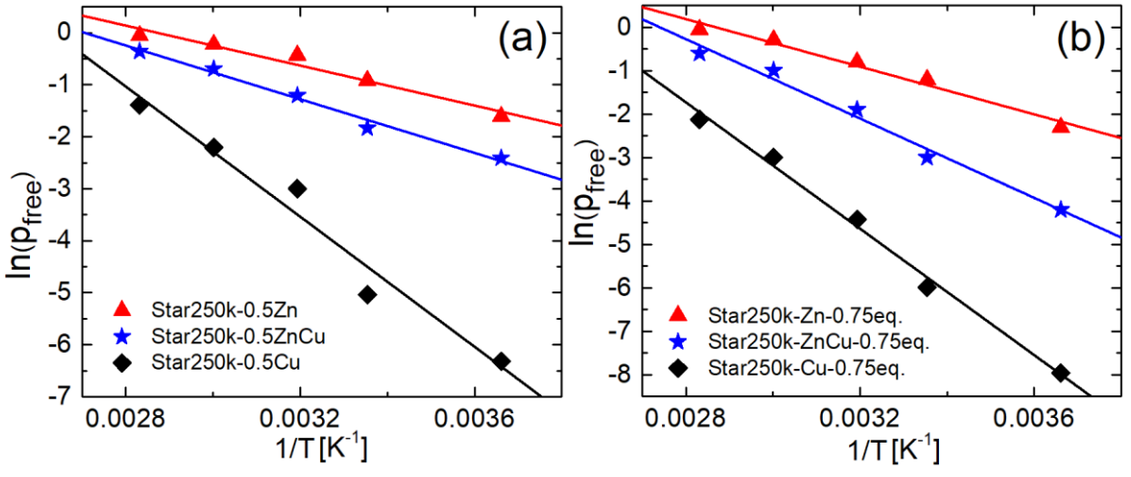

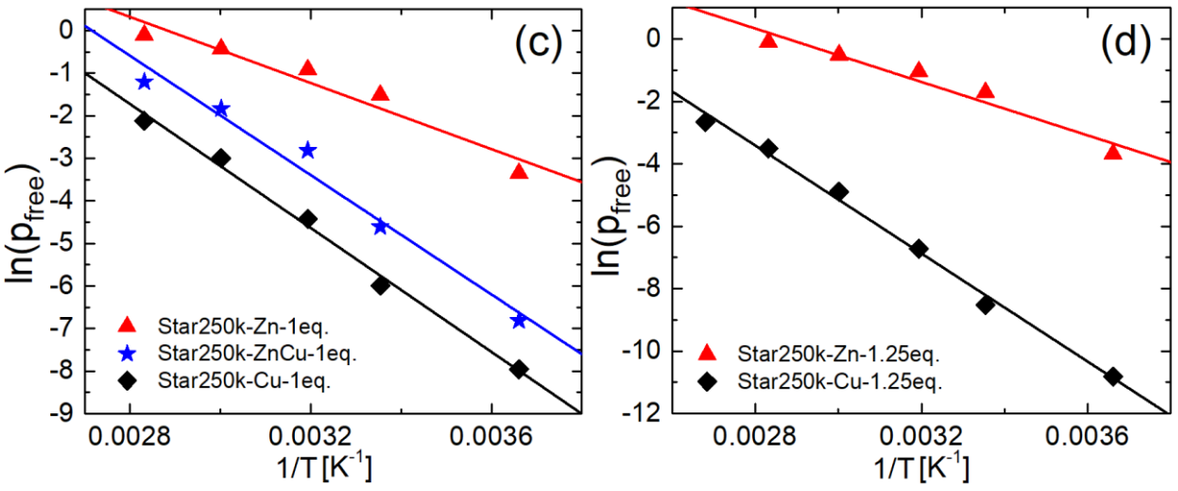

Figure 17. Values of the fraction of time when stickers are unassociated, p_{free}, for Star250k single and double dynamics networks as functions of inverse temperature at (a) 0.5eq., (b) 0.75eq., (c)1.0eq. and (d) 1.25 eq..

From the data in Figure 17, the activation energy E_a at different ion contents can be determined by considering:

$$p_{free}(T) = p_{free}(T = 25℃)e^{-\frac{E_a}{RT}} \quad (12)$$

It should be highlighted however that the extracted activation energy for both single and double dynamics networks is not directly related to the association energy of bis-complexes, since the association time for bis-complexes, terpyridine-Zn(II) or terpyridine-Cu(II), is unknown at each temperature. It rather reflects the average influence of the sticker dynamics due to ligand exchange mechanisms and/or the influence of both the dissociation and association mechanisms of the stickers, which is expected to depend on the relative importance of τ_{free} compared to the disentanglement time of a free arm.

The extracted activation energy are plotted as function of ion content in Figure 18. Upon increasing ion content, the activation energy for both single and double dynamics networks increases, which

confirms that the temperature has a larger effect on the viscoelastic response at higher crosslinking density. We also observe that the activation energy of the double dynamics network has a stronger dependence; it varies from a value similar to the single dynamic network containing Zn(II) ions to a value similar to the single dynamic network containing Cu(II) ions when the ions are added in excess.

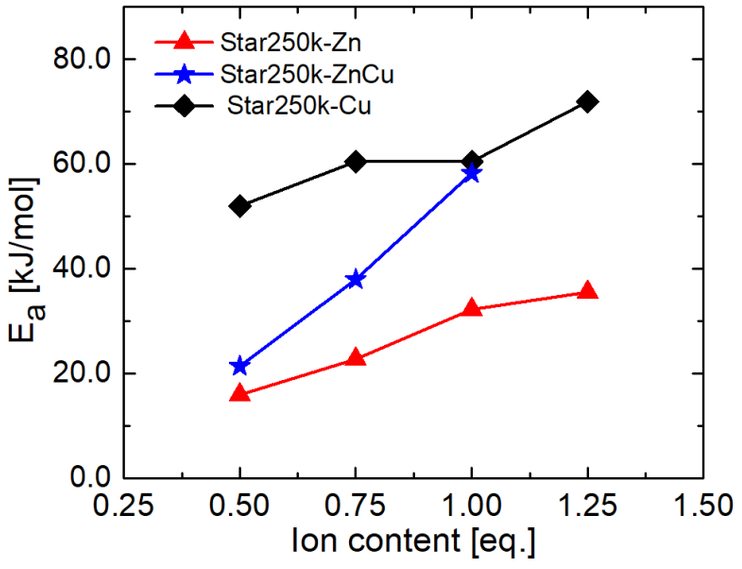

Figure 18. Activation energy for Star250k single- and double dynamics networks as function of ion content

While for these networks the influence of the stickers is only known as an average effect, an estimation of τ_{free} is nevertheless possible for the transient network containing Cu(II) ions at 0 °C. In this specific case, both p_{free} and $\tau_{sticker}$, can be estimated from the creep measurements and from Equations 9,10 and 11. For example, it is found that $\tau_{free} \cong 0.05$s for 1.0eq.Cu and $\tau_{free} \cong 0.01$s for 1.25eq.Cu, which is much shorter than the time necessary for a free arm to relax (t ≅ 3.33s, at the terminal crossover frequency of 0.3rad/s for Star250k reference sample at 0°C). This confirms that a sticker has to dissociate and re-associate several times before the complete disentanglement of the building blocks (arms) takes place.

As shown in Figure 16.c, the lifetime of tpy-Zn(II) complexes, $\tau_{sticker,}$ can also be determined at 0 °C, at the inverse frequency where the viscoelastic curves start to deviate from those of the other transient networks. For example, it is equal to around 0.25s with 1.0eq. Zn(II) (see Figure 16.c). The corresponding value of τ_{free} for networks with Zn(II) at 0°C can then be calculated from Equation 11. The values found for the different systems are shown in Figure 19. It can be observed that τ_{free} decreases with increasing the ion content, presumably, because of the larger density of ions in the surrounding of a specific ligand.

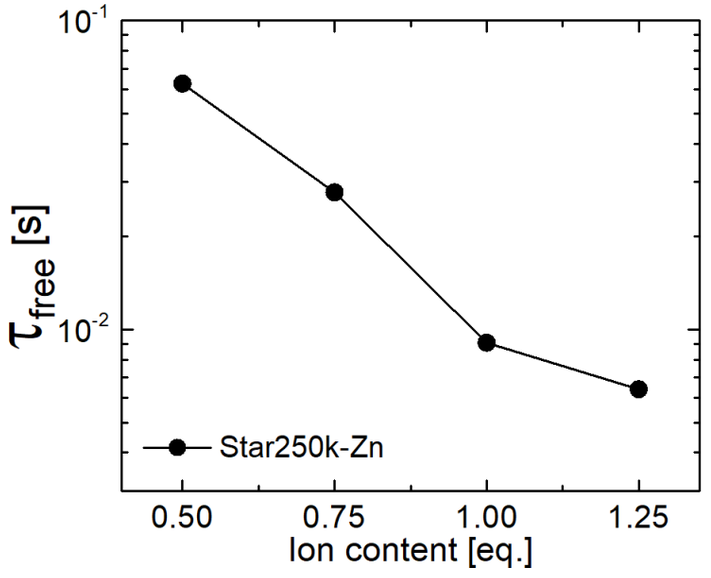

Figure 19: Estimated values of dissociated stickers lifetime τ_{free} as a function of Zn(II) ion contents at 0 °C.

CONCLUSIONS

In this work, we report on the rational analysis of the linear viscoelastic properties of single and double dynamics networks based on two metal-ligand crosslinks of different lifetime, terpyridine-Zn(II) and/or terpyridine-Cu(II) coupled with telechelic four-arm stars PnBA. We have studied systematically, experimentally and theoretically, the linear viscoelastic spectra of the networks. Both single and double dynamics networks exhibit a multi-scale behavior with the metal-ligand transient crosslinks acting as

extra friction points at chain extremities yielding an overall delay of the telechelic arm relaxation process. In particular, an averaged cooperative behavior for describing the sticker dynamics of double dynamics networks is revealed rather than discrete contributions of each metal-ligand transient crosslinks. The relaxation behavior of blends lies between of two single dynamic networks, and gradually shifts from the behavior closer to the weaker one (Zn(II)) at stoichiometric ion amount to properties closer to the stronger one (Cu(II)) at excess ion amount, due to the fact that tpy-Cu(II) complexes play a dominant role in double dynamics networks. We have modeled the linear viscoelasticity of these associating networks by accounting for both association/dissociation dynamics of metal-ligand crosslinks and the entanglement dynamics. Our model describes the experimental data accurately, based on two fit parameters, p_{dang} (the fraction of dangling ends) and p_{free} (the average probability for a sticker to remain free). This has allowed us to identify the presence of a certain fraction of dangling ends in the networks at both stoichiometric amount and even at excessive ion content, and to determine the association probability of the complexes, leading to an improved understanding of the properties of these topologically complex transient networks. The values of the parameter p_{free} follow an Arrhenius dependence with temperature and gradually decrease with increasing ion content. From this dependence, an activation energy could be extracted, which represents the average global effect of the stickers on chain dynamics. In conclusion, this work shows that using one or two types of metal-ligand crosslinks within the same parent material yields a wide range of material response and opens the route to tailor their viscoelastic properties. Further studies on nonlinear shear and extensional rheology will be necessary to better understand the entire spectrum of properties and potential applications of these materials.

Acknowledgments

Financial support by the EU (Horizon 2020, Marie Skłodowska-Curie ITN DoDyNet, Grand Agreement No. 765811) is gratefully acknowledged. EVR is Senior Research Associated of the FNRS.

References

(1) Enke, M.; Bode, S.; Vitz, J.; Schacher, F. H.; Harrington, M. J.; Hager, M. D.; Schubert, U. S. Self-Healing Response in Supramolecular Polymers Based on Reversible Zinc−histidine Interactions. Polymer 2015, 69, 274−282.

(2) Byette, F.; Laventure, A.; Marcotte, I.; Pellerin, C. Metal–Ligand Interactions and Salt Bridges as Sacrificial Bonds in Mussel Byssus-Derived Materials. Biomacromolecules 2016, 17(10), 3277–3286.

(3) Brassinne, J.; Fustin, C.-A.; Gohy, J.-F. Polymer Gels Constructed Through Metal–Ligand Coordination. Journal of Inorganic and Organometallic Polymers and Materials 2012, 23(1), 24–40.

(4) Shi L. Y.; Ding P. H.; Wang Y. Z.; Zhang Y., Ossipov D.; Hilborn J. Self-Healing Polymeric Hydrogel Formed by Metal–Ligand Coordination Assembly: Design, Fabrication, and Biomedical Applications. Macromol. Rapid Commun. 2019, 1800837, 1-18.

(5) Riccardi, L.; Genna, V.; De Vivo, M. Metal–ligand interactions in drug design. Nature Reviews Chemistry 2018, 2(7), 100–112.

(6) Winter, A.; Schubert, U. S. Synthesis and characterization of metallo-supramolecular polymers. Chemical Society Reviews 2016, 45(19), 5311–5357.

(7) Staropoli, M.; Raba, A.; Hövelmann, C. H.; Krutyeva, M.; Allgaier, J.; Appavou, M.-S.; Keiderling U.; Stadler F. J.; Pyckhout-Hintzen W.; Wischnewski A.; Richter, D. Hydrogen Bonding in a Reversible Comb Polymer Architecture: A Microscopic and Macroscopic Investigation. Macromolecules 2016, 49(15), 5692–5703.

(8) Jangizehi, A.; Ghaffarian, S. R.; Ahmadi, M. Dynamics of entangled supramolecular polymer networks in presence of high-order associations of strong hydrogen bonding groups. Polymers for Advanced Technologies 2017, 29(2), 726–735.

(9) Zhang, Z. J.; Liu, C.; Cao, X.; Gao, L. C.; Chen, Q. Linear Viscoelastic and Dielectric Properties of Strongly Hydrogen-Bonded Polymers near the Sol–Gel Transition. Macromolecules 2016, 49(23), 9192–9202.

(10) Register, R. A. Morphology and Structure–Property Relationships in Random Ionomers: Two Foundational Articles from Macromolecules. Macromolecules 2020, 53(5), 1523–1526.

(11) Chen, Q.; Tudryn, G. J.; Colby, R. H. Ionomer dynamics and the sticky Rouse model. Journal of Rheology 2013, 57(5), 1441–1462.

(12) Pu, W. F.; Jiang, F.; Wei, B.; Tang, Y. L.; He, Y. Y. A gel-like comb micro-block hydrophobic associating polymer: Synthesis, solution property and the sol-gel transition at semi-dilute region. Macromolecular Research 2017, 25(2), 151–157.

(13) Aubry, T.; Moan, M. Rheological behavior of a hydrophobically associating water soluble polymer. Journal of Rheology 1994, 38(6), 1681-1692.

(14) Noro, A.; Hayashi, M.; Matsushita, Y. Design and properties of supramolecular polymer gels. Soft Matter 2012, 8(24), 6416-6429.

(15) McConnell, A. J.; Wood, C. S.; Neelakandan, P. P.; Nitschke, J. R. Stimuli-Responsive Metal–Ligand Assemblies. Chemical Reviews 2015, 115(15), 7729–7793.

(16) Beck, J. Benjamin; Ineman, Jennifer M.; Rowan, Stuart J. Metal/Ligand-Induced Formation of Metallo-Supramolecular Polymers. Macromolecules 2005, 38(12), 5060–5068.

(17) Mozhdehi, D.; Neal, J. A.; Grindy, S. C.; Cordeau, Y.; Ayala, S.; Holten-Andersen, N.; Guan, Z. B. Tuning Dynamic Mechanical Response in Metallopolymer Networks through Simultaneous Control of Structural and Temporal Properties of the Networks. Macromolecules 2016, 49(17), 6310–6321.

(18) Loveless, D. M.; Jeon, S. L.; Craig, S. L. Rational Control of Viscoelastic Properties in Multicomponent Associative Polymer Networks. Macromolecules 2005, 38(24), 10171–10177.

(19) Yount, W. C.; Loveless, D. M.; Craig, S. L. Small-Molecule Dynamics and Mechanisms Underlying the Macroscopic Mechanical Properties of Coordinatively Crosslinked Polymer Networks. Journal of the American Chemical Society 2005, 127(41), 14488–14496.

(20) Guillet, P., Mugemana, C., Stadler, F. J., Schubert, U. S., Fustin, C.-A., Bailly, C., Gohy, J.-F. Connecting micelles by metallo-supramolecular interactions: towards stimuli responsive hierarchical materials. Soft Matter, 2009, 5(18), 3409-3411.

(21) Brassinne, J.; Stevens, A. M.; Van Ruymbeke, E.; Gohy, J.-F.; Fustin, C.-A. Hydrogels with Dual Relaxation and Two-Step Gel–Sol Transition from Heterotelechelic Polymers. Macromolecules 2013, 46(22), 9134–9143.

(22) Nair, K. P.; Breedveld, V.; Weck, M. Multiresponsive Reversible Polymer Networks Based on Hydrogen Bonding and Metal Coordination. Macromolecules 2011, 44(9), 3346–3357.

(23) Narita, T.; Mayumi, K.; Ducouret, G.; Hébraud, P. Viscoelastic Properties of Poly(vinyl alcohol) Hydrogels Having Permanent and Transient Crosslinks Studied by Microrheology, Classical Rheometry, and Dynamic Light Scattering. Macromolecules 2013, 46(10), 4174–4183.

(24) Yang, H.; Ghiassinejad, S.; van Ruymbeke, E.; Fustin, C.-A. Tunable Interpenetrating Polymer Network Hydrogels Based on Dynamic Covalent Bonds and Metal-Ligand Bonds. Macromolecules 2020, 53, 16, 6956–6967.

(25) Grindy, S. C.; Learsch, R.; Mozhdehi, D.; Cheng, J.; Barrett, D. G.; Guan, Z. B.; Messersmith P. B.; Holten-Andersen, N. Control of hierarchical polymer mechanics with bioinspired metal-coordination dynamics. Nature Materials 2015, 14(12), 1210–1216.

(26) Kobayashi, Y.; Hirase, T.; Takashima, Y.; Harada, A.; Yamaguchi, H. Self-healing and shape-memory properties of polymeric materials crosslinked by hydrogen bonding and metal–ligand interactions. Polymer Chemistry 2019, 10, 4519-4523.

(27) Dutta, A.; Das, R. K. Dual Crosslinked Hydrogels with High Strength, Toughness, and Rapid Self-Recovery Using Dynamic Metal-Ligand Interactions. Macromolecular Materials and Engineering 2019, 304(8), 1900195.

(28) Wang, Z. H., Xie, C., Yu, C. J., Fei, G. X., Wang, Z. H., Xia, H. S. A Facile Strategy for Self-Healing Polyurethanes Containing Multiple Metal-Ligand Bonds. Macromolecular Rapid Communications 2018, 39(6), 1700678.

(29) Grindy, S. C.; Lenz, M.; Holten-Andersen, N. Engineering Elasticity and Relaxation Time in Metal-Coordinate Cross-Linked Hydrogels. Macromolecules 2016, 49(21), 8306–8312.

(30) Fullenkamp, Dominic E.; He, Lihong; Barrett, Devin G.; Burghardt, Wesley R.; Messersmith, Phillip B. Mussel-Inspired Histidine-Based Transient Network Metal Coordination Hydrogels. Macromolecules 2013, 46(3), 1167–1174.

(31) Cazzell, S. A.; Holten-Andersen, N.. Expanding the Stoichiometric Window for metal cross-linked gel assembly using competition. Proc. Natl. Acad. Sci. USA. 2019, 116 (43), 21369-21374.

(32) Schmolke, Willi; Ahmadi, Mostafa; Seiffert, Sebastian. Enhancement of Metallo-supramolecular Dissociation Kinetics in Telechelic Terpyridine-capped Poly(ethylene glycol) Assemblies in the Semi-Dilute Regime. Phys. Chem. Chem. Phys. 2019, 21, 19623-19638.

(33) van Ruymbeke, E.; Vlassopoulos, D.; Mierzwa, M.; Pakula, T.; Charalabidis, D.; Pitsikalis, M.; Hadjichristidis, N. Rheology and Structure of Entangled Telechelic Linear and Star Polyisoprene Melts. Macromolecules 2010, 43(9), 4401–4411.

(34) Zhuge, F.; Brassinne, J.; Fustin, C.-A.; van Ruymbeke, E.; Gohy, J.-F. Synthesis and Rheology of Bulk Metallo-Supramolecular Polymers from Telechelic Entangled Precursors. Macromolecules 2017, 50(13), 5165–5175.

(35) Zhuge, F.; Hawke, L. G. D.; Fustin, C.-A.; Gohy, J.-F.; van Ruymbeke, E. Decoding the linear viscoelastic properties of model telechelic metallo-supramolecular polymers. Journal of Rheology 2017, 61(6), 1245–1262.

(36) van Ruymbeke, E.; Keunings, R.; Bailly, C. Prediction of linear viscoelastic properties for polydisperse mixtures of entangled star and linear polymers: Modified tube-based model and comparison with experimental results. Journal of Non-Newtonian Fluid Mechanics 2005, 128(1), 7–22.

(37) van Ruymbeke, E.; Bailly, C.; Keunings, R.; Vlassopoulos, D. A General Methodology to Predict the Linear Rheology of Branched Polymers. Macromolecules 2006, 39(18), 6248–6259.

(38) John D. Ferry. Viscoelastic Properties of Polymers, 3rd Edition. (Wiley, 1980).

(39) Honerkamp, J. & Weese, J. A nonlinear regularization method for the calculation of relaxation spectra. Rheol. Acta 1993, 32, 65–73.

(40) van Ruymbeke, E., E. B. Muliawan, D. Vlassopoulos, H. Gao, and K. Matyjaszewski, Melt rheology of star polymers with large number of small arms, prepared by crosslinking poly(n-butyl acrylate) macromonomers via ATRP. Eur. Polym. J 2011, 47, 746–751.

(41) Walsh, D., P. Zoller, Standard Pressure-Volume-Temperature Data for Polymers, CRC, Lancaster, 1995.

(42) Schwarzl, F. R. Numerical calculation of storage and loss modulus from stress relaxation data for linear viscoelastic materials. Rheol. Acta 1971, 10, 165−173.

(43) Lewis, R., Malic, N., Saito, K., Evans, R. A., and Cameron, N. R. Ultra-High Molecular Weight Linear Coordination Polymers with Terpyridine Ligands. Chemical Science 2019, 10, 6174–6183.

(44) Amin, D., A. E. Likhtman, and Z. Wang, Dynamics in supramolecular polymer networks formed by associating telechelic chains. Macromolecules 2016, 49, 7510–7524.

(45) S. Schneider, G. Brehm, C.-J. Prenzel, W. Jäger, M. I. Silva, H. D. Burrows, S. T. Formosinho. Vibrational Spectra, Normal Coordinate Analysis and Excited-State Lifetimes for a Series of Polypyridylruthenium(II) Complexes. Journal of Raman Spectroscopy 1996, 27, 163-175.

(46) Lohmeijer, B.G.G., Playing LEGO with macromolecules: connecting polymer chains using terpyridine metal complexes, PhD thesis, Eindhoven University of Technology, 2004.

(47) Yesilyurt, Volkan; Ayoob, Andrew M.; Appel, Eric A.; Borenstein, Jeffrey T.; Langer, Robert; Anderson, Daniel G.. Mixed Reversible Covalent Crosslink Kinetics Enable Precise, Hierarchical Mechanical Tuning of Hydrogel Networks. Advanced Materials 2017, 29(19), 1605947.

(48) Chen, H.; Zhang, J.; Yu, W.; Cao, Y.; Cao, Z.; Tan, Y.. Control Viscoelasticity of Polymer Networks with Crosslinks of Superposed Fast and Slow Dynamics. Angewandte Chemie International Edition 2021, 60(41), 22332-22338.

(49) Holyer, R. H., Hubbard, C. D., Kettle, S. F. A., and Wilkins, R. G.. The Kinetics of Replacement Reactions of Complexes of the Transition Metals with 2,2',2"-Terpyridine. Inorganic Chemistry 1966, 5(4), 622–625.

(50) Rosario Cali, Enrico Rizzarelli, Silvio Sammartano and Giuseppe Siracusa. Thermodynamics of 2,2':6',2"-Terpyridinecopper(II) complexes in aqueous solution. Transition Metal Chemistry 1979, 4(5), 328–332.

(51) Philip R. Andres; Harald Hofmeier; Ulrich S. Schubert. Complexation Parameters of Terpyridine-Metal Complexes. ACS Symposium Series, 2006, 928, 141-156.

Journal of Rheology

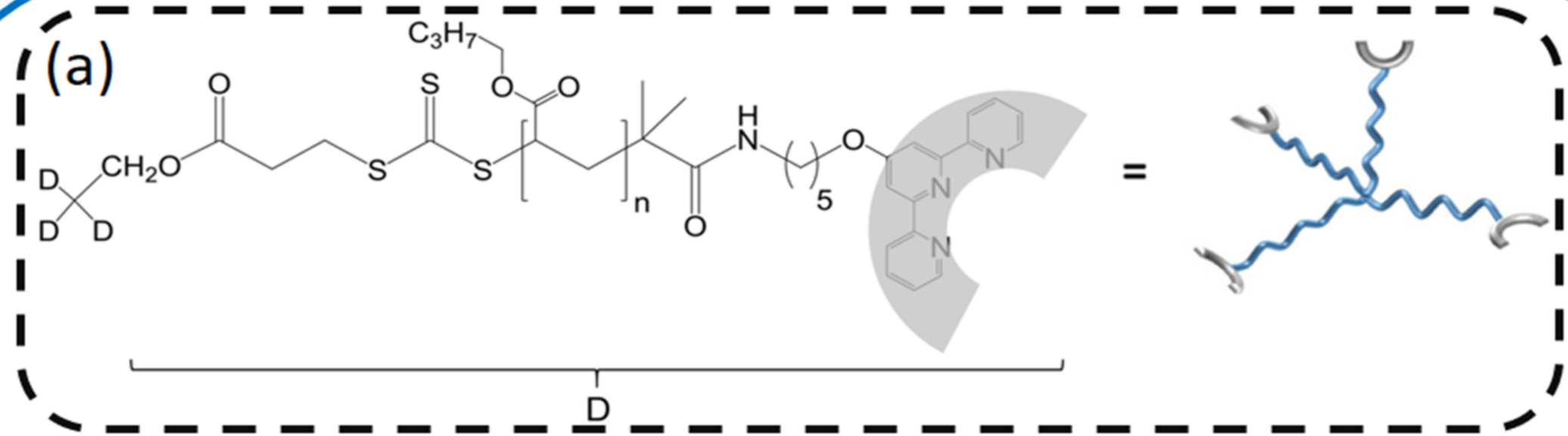

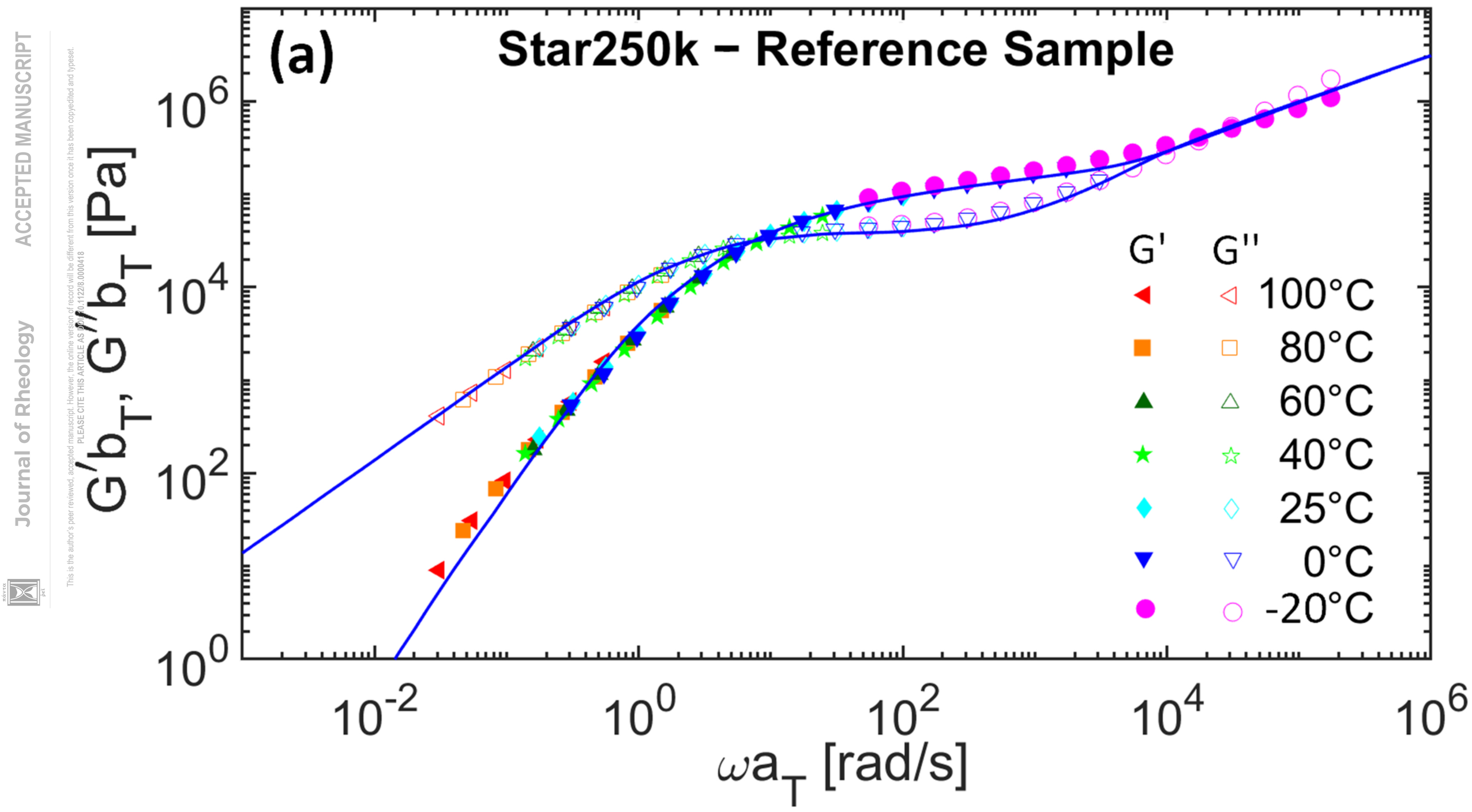

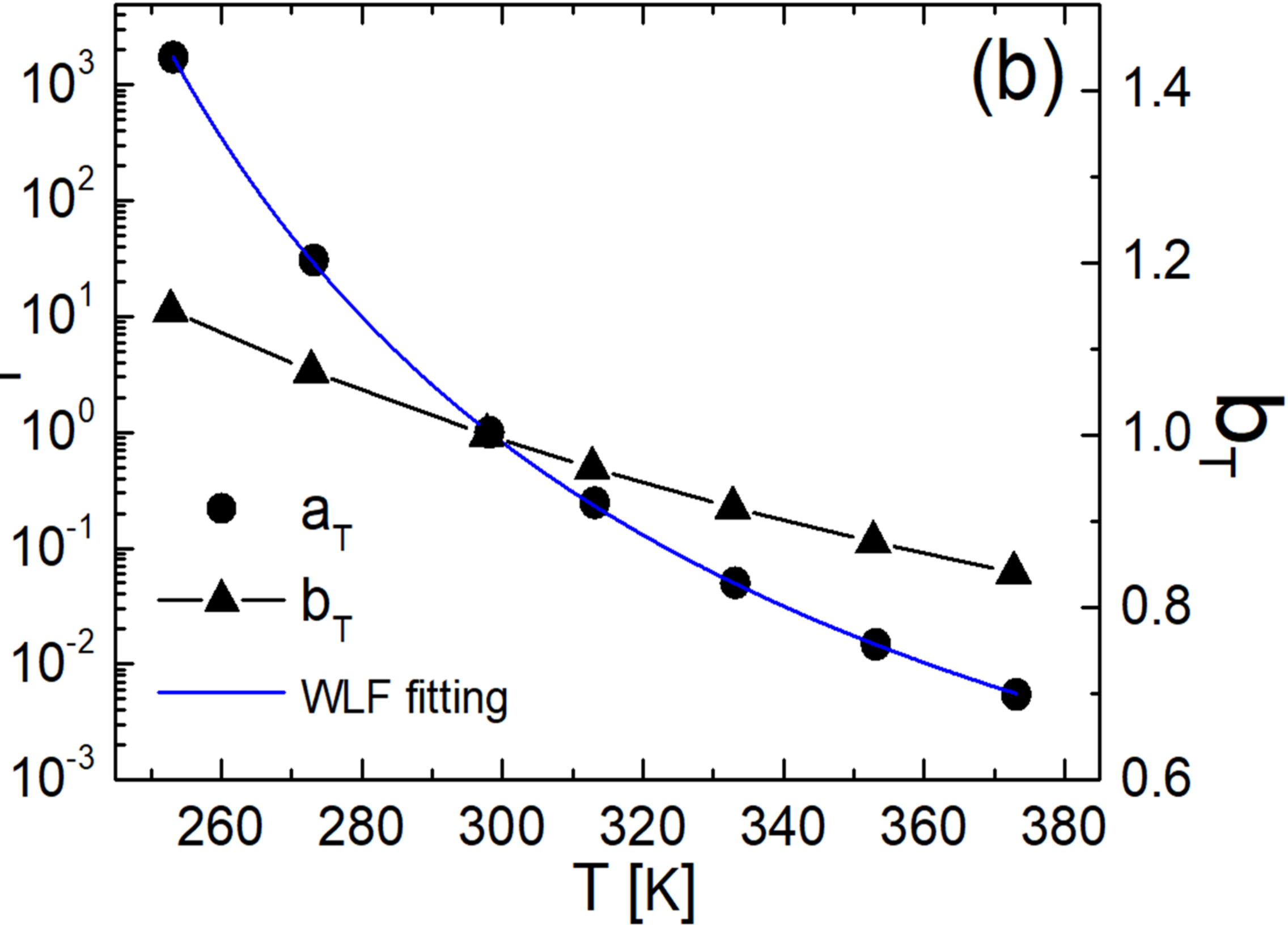

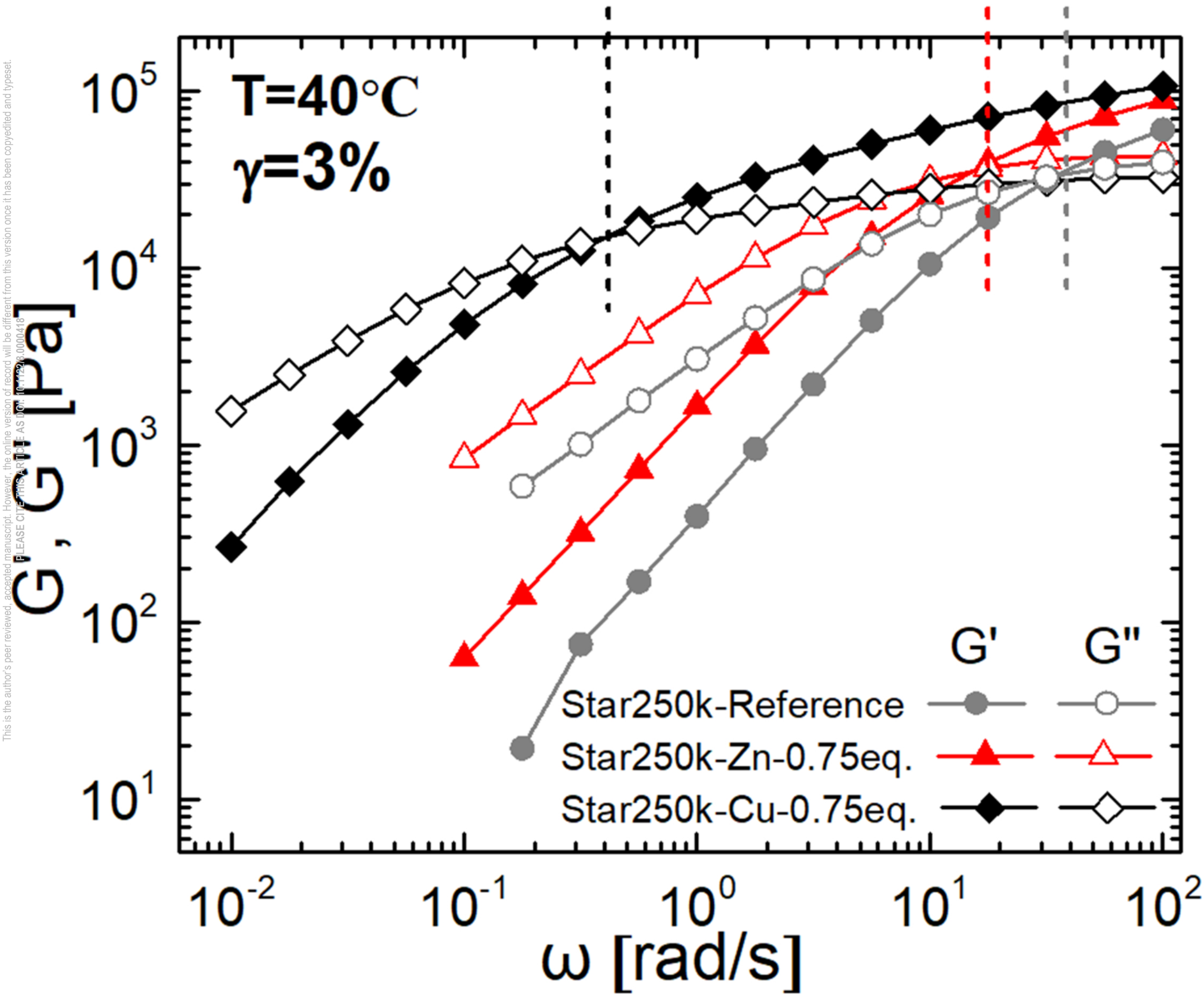

Journal of Rheology

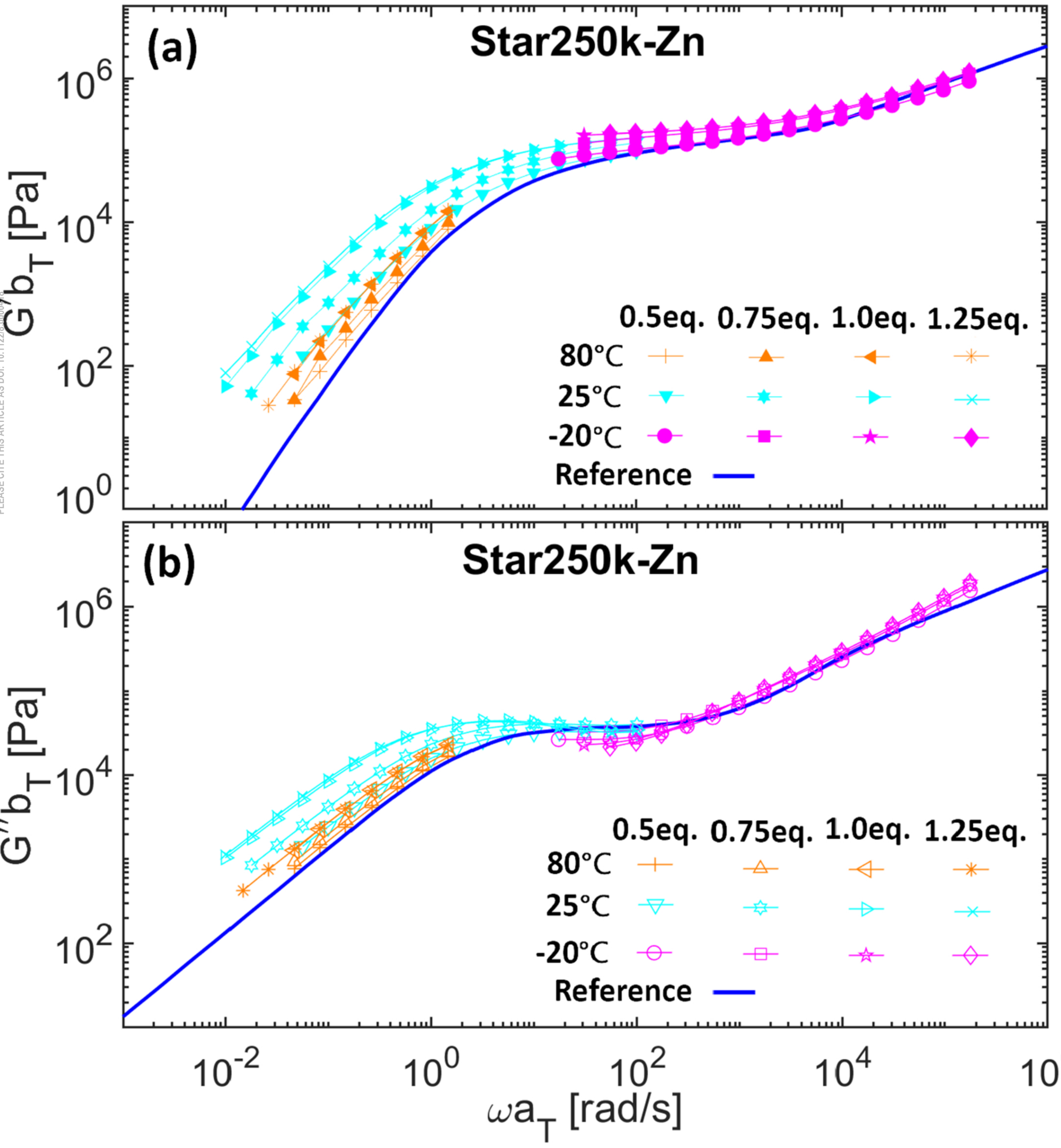

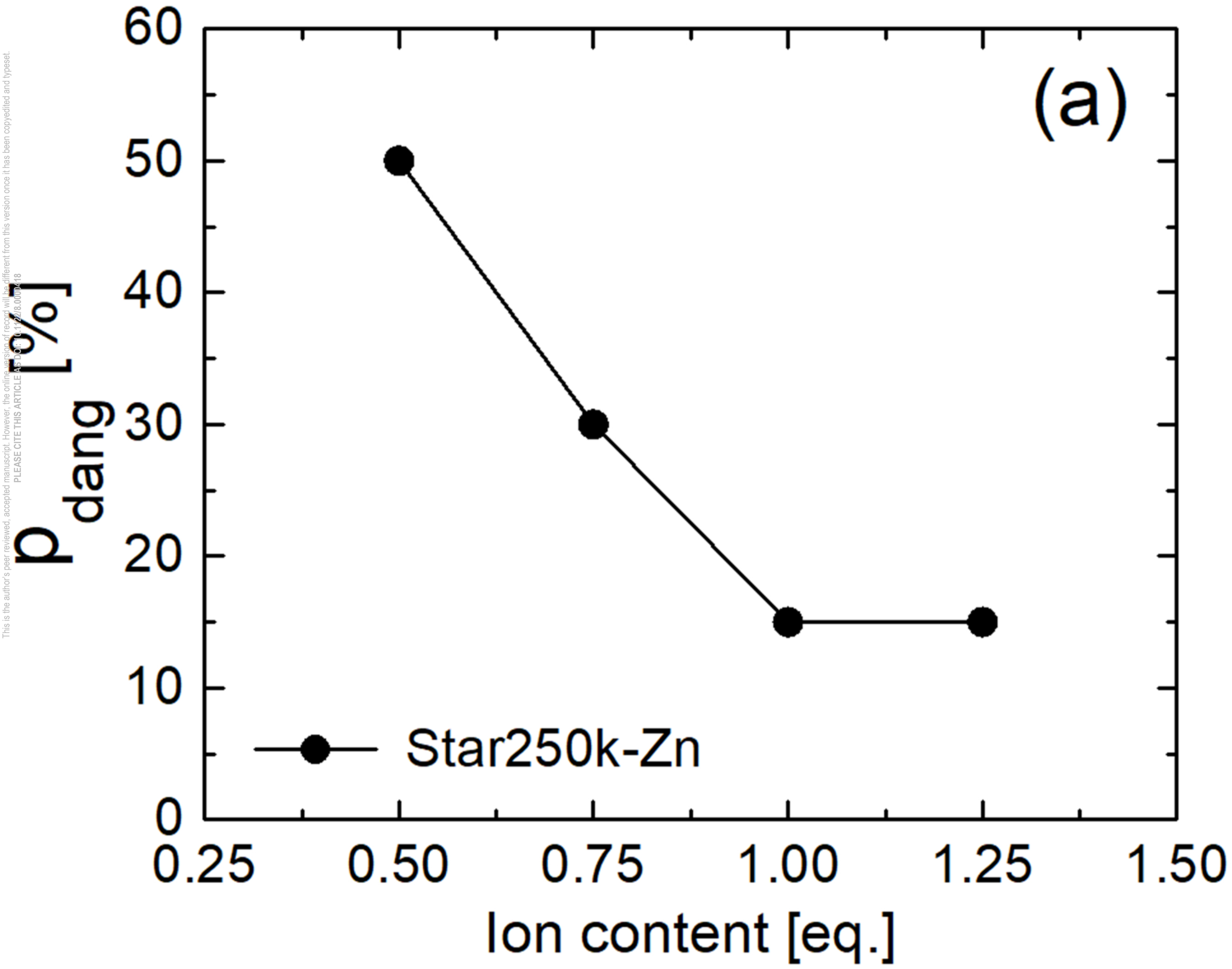

Journal of Rheology

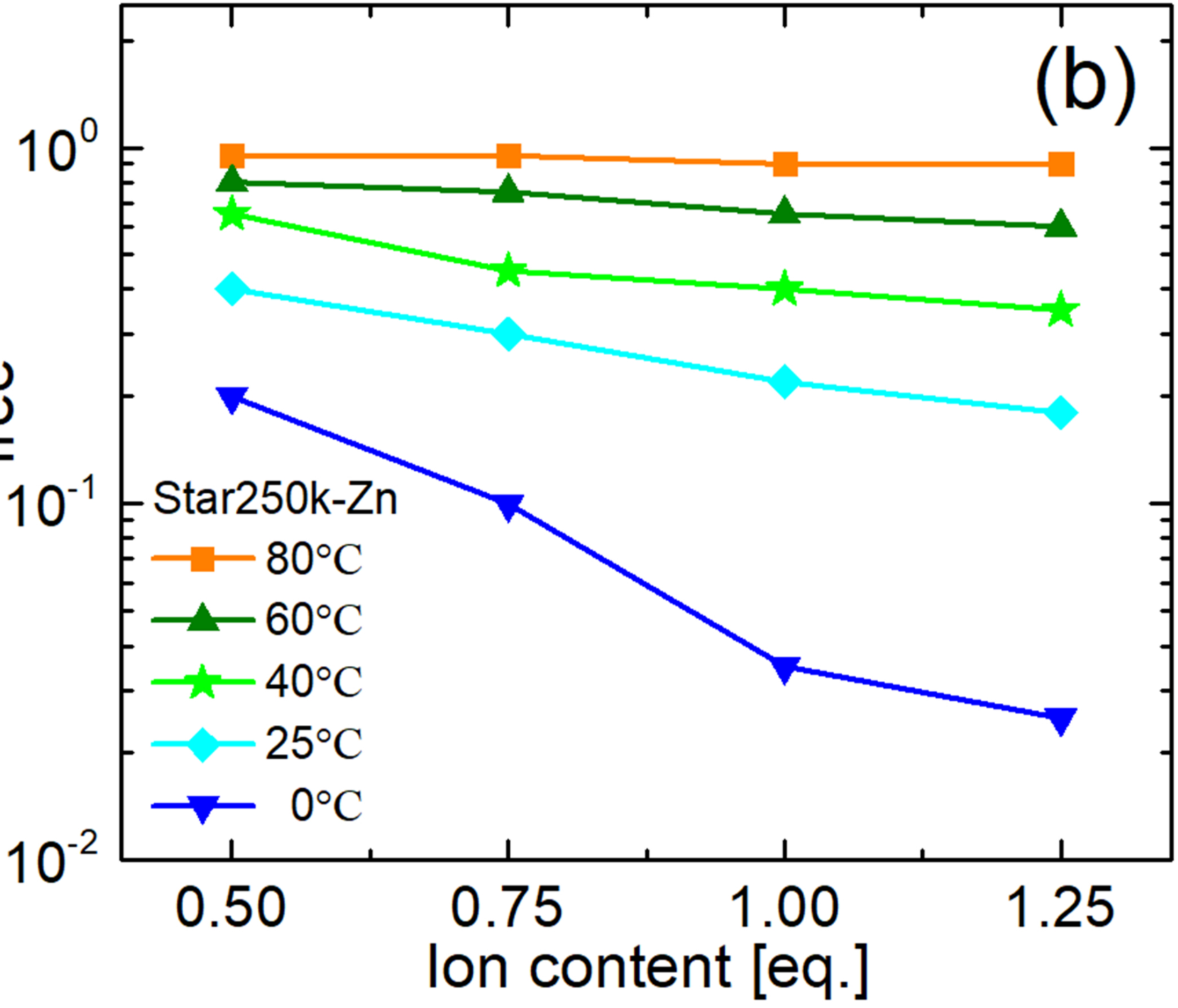

Journal of Rheology

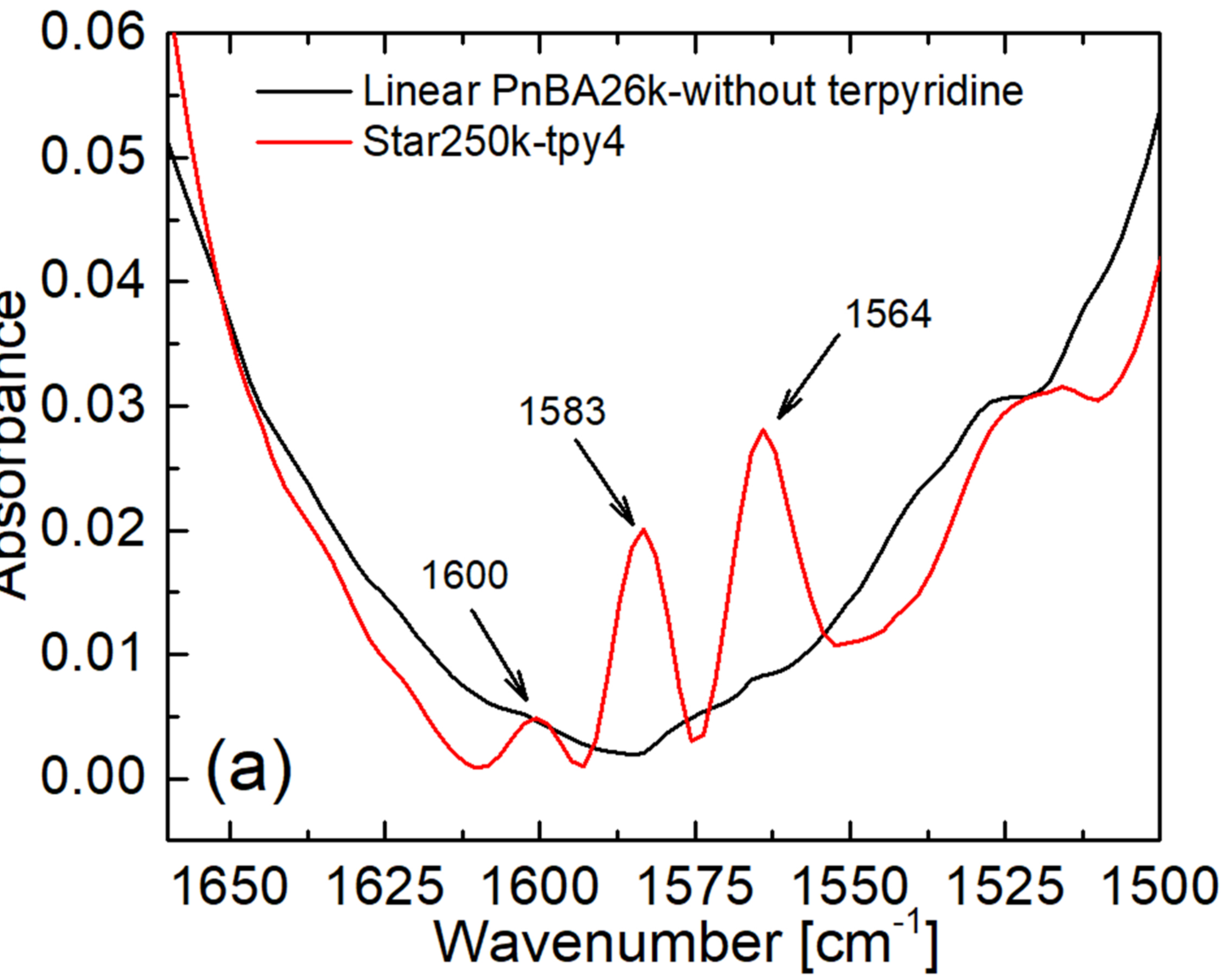

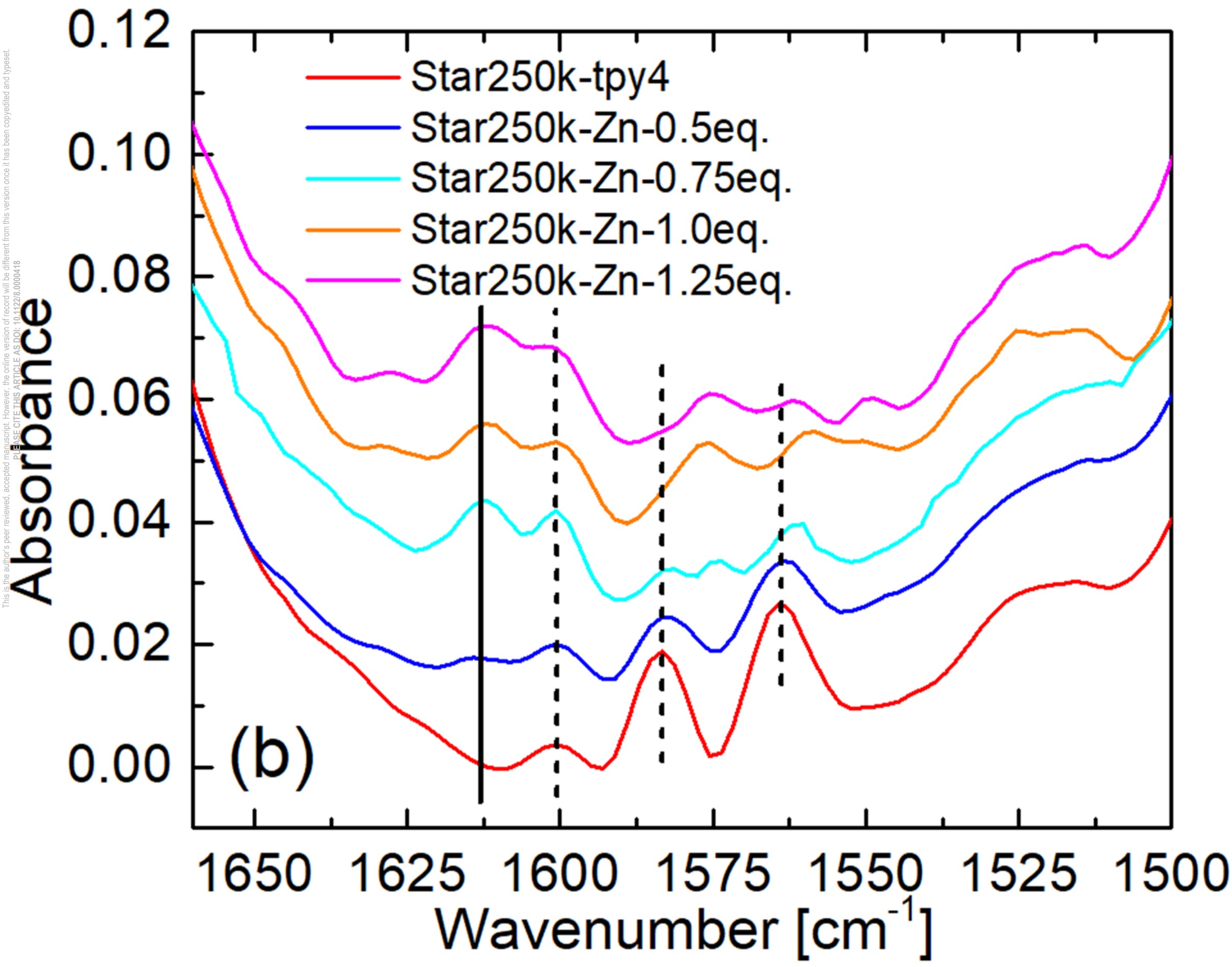

Journal of Rheology

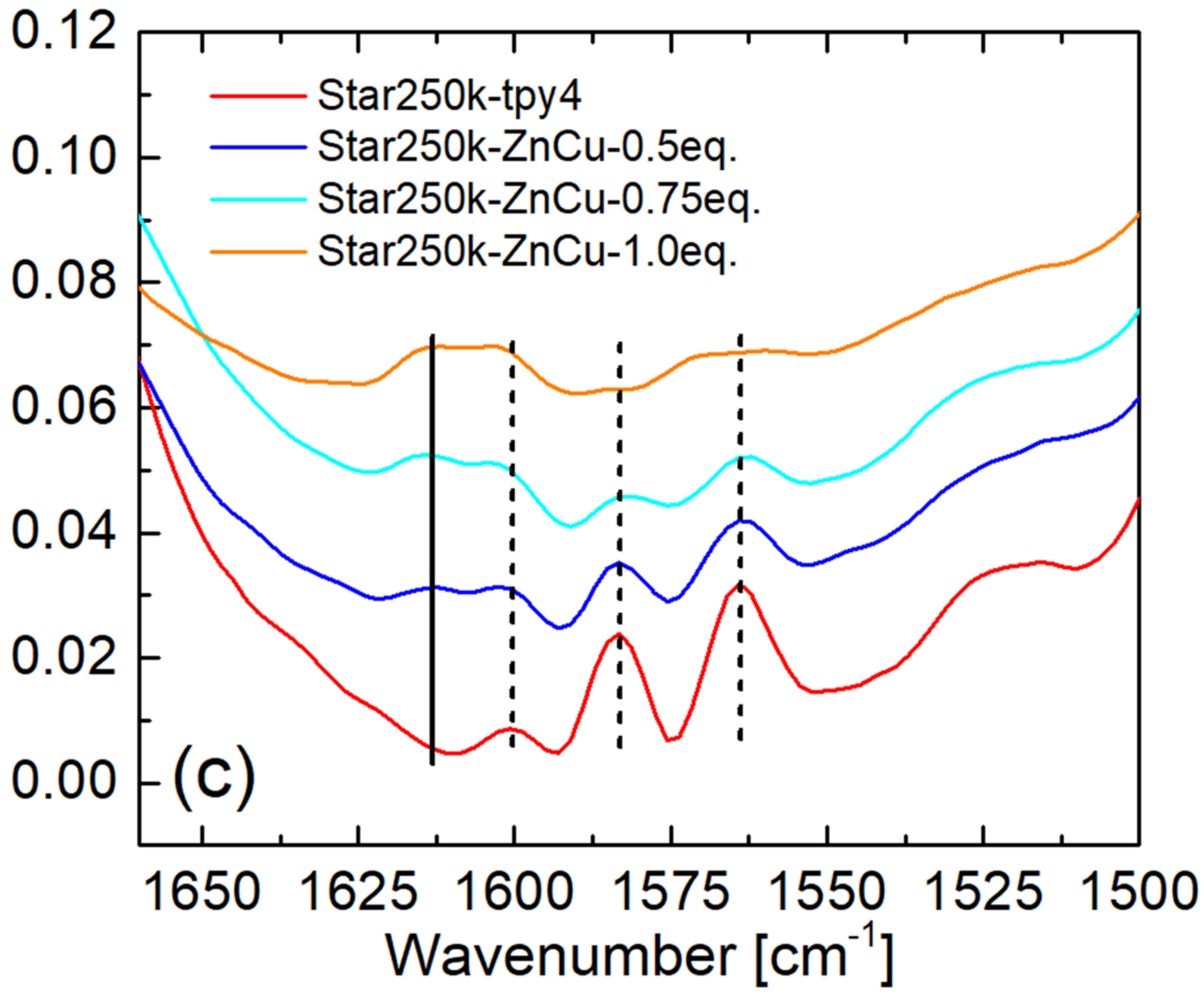

Journal of Rheology

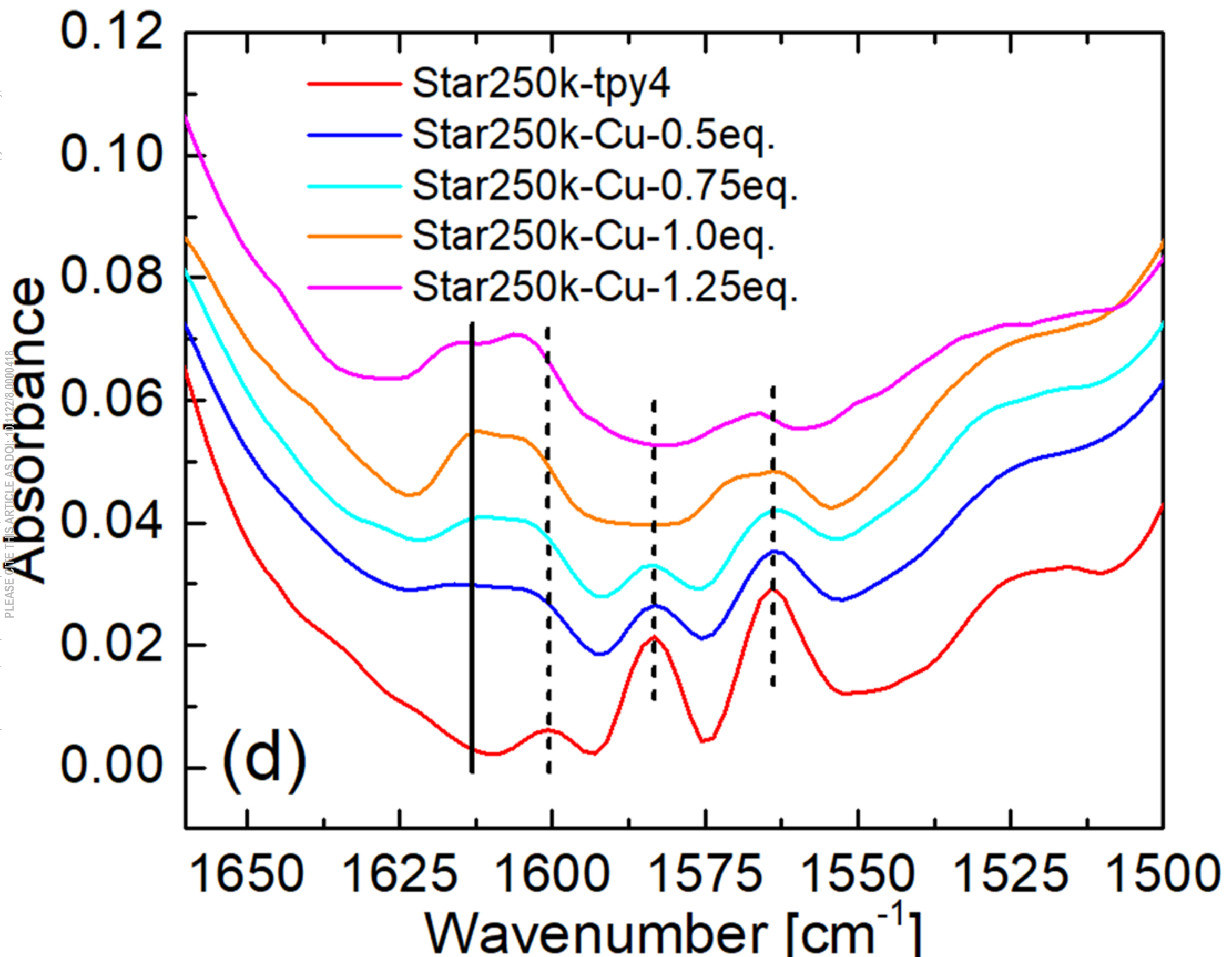

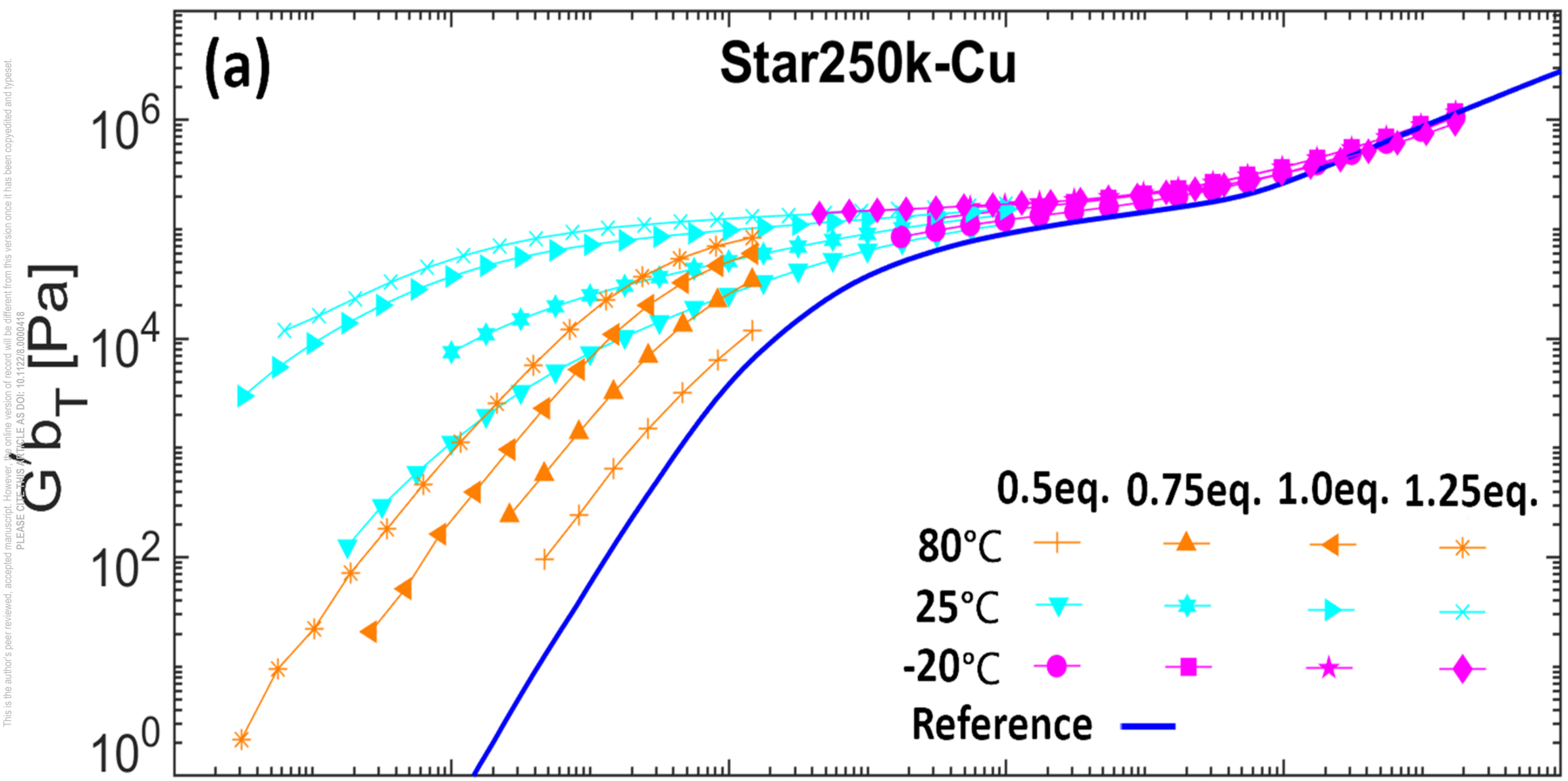

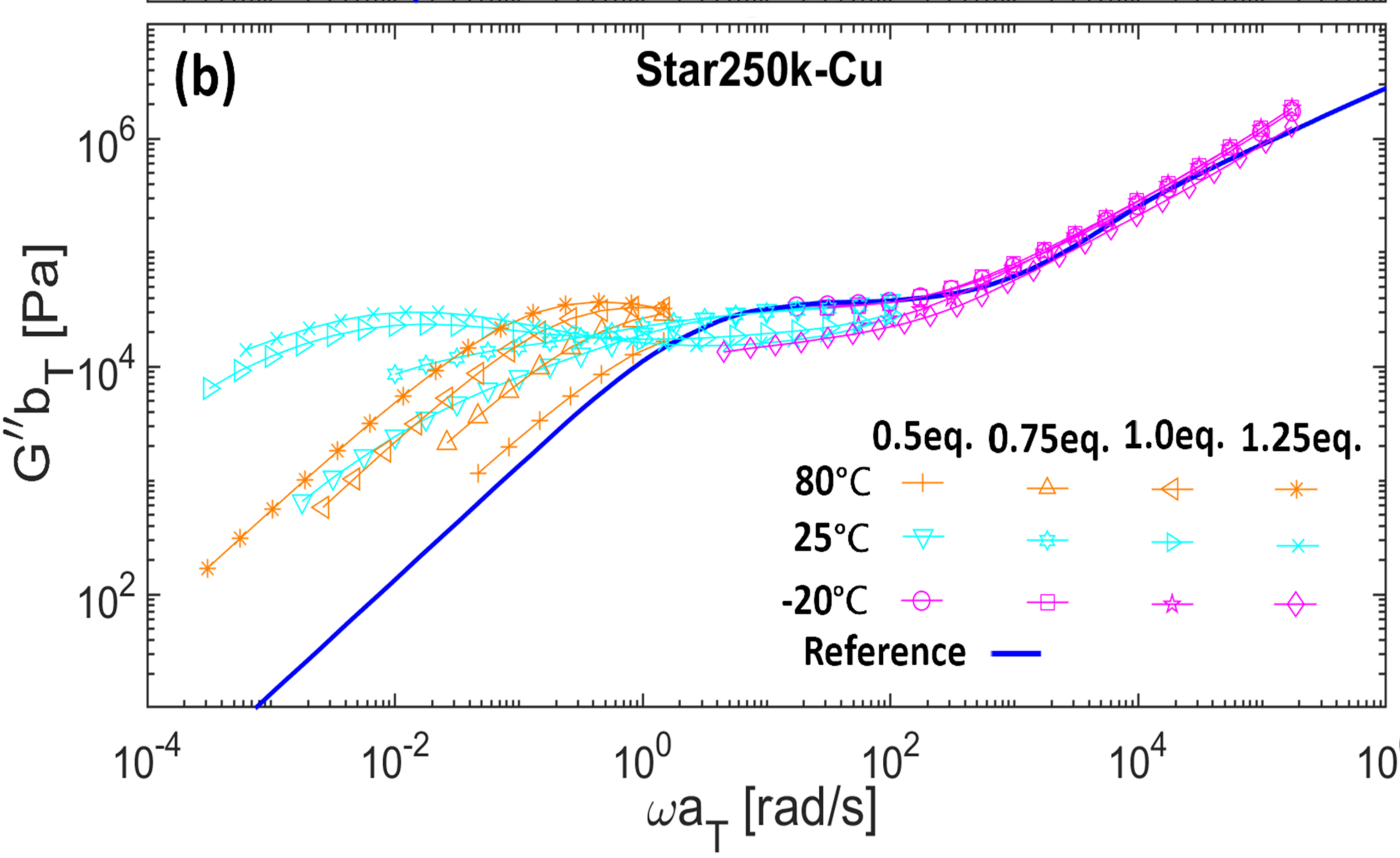

(a) Star250k−Cu−0.50 eq.

$G'b_T$, $G''b_T$ [Pa]

p_{dang}=0.6

G'	G''		p_{free}
■	□	80℃	0.25
▲	△	60℃	0.11
★	☆	40℃	0.05
♦	◇	25℃	0.0065
▼	▽	0℃	0.0018

(b) Star250k−Cu−0.75 eq.

$G'b_T$, $G''b_T$ [Pa]

p_{dang}=0.35

G'	G''		p_{free}
■	□	80℃	0.12
▲	△	60℃	0.05
★	☆	40℃	0.012
♦	◇	25℃	0.0025
▼	▽	0℃	0.0004

(c) Star250k−Cu−1.0 eq.

$G'b_T$, $G''b_T$ [Pa]

p_{dang}=0.25

G'	G''		p_{free}
■	□	80℃	0.06
▲	△	60℃	0.018
★	☆	40℃	0.0026
♦	◇	25℃	0.0004
▼	▽	0℃	0.0001

(d) Star250k−Cu−1.25 eq.

$G'b_T$, $G''b_T$ [Pa]

pdang=0.2

G'	G''		pfree
◀	◁	100°C	0.07
■	□	80°C	0.03
▲	△	60°C	0.0075
★	☆	40°C	0.0012
♦	◇	25°C	0.0002
▼	▽	0°C	0.00002

ωa_T [rad/s]

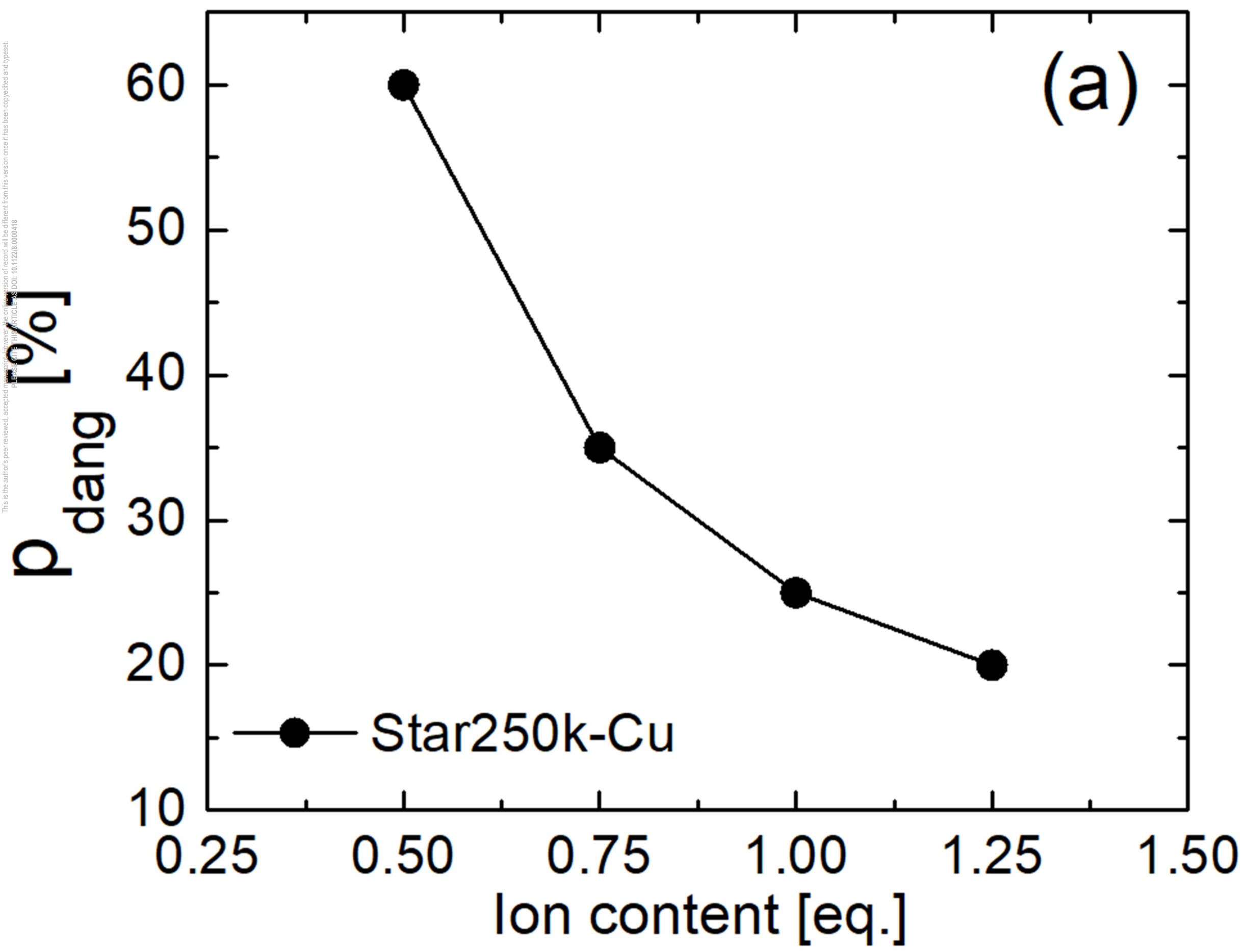

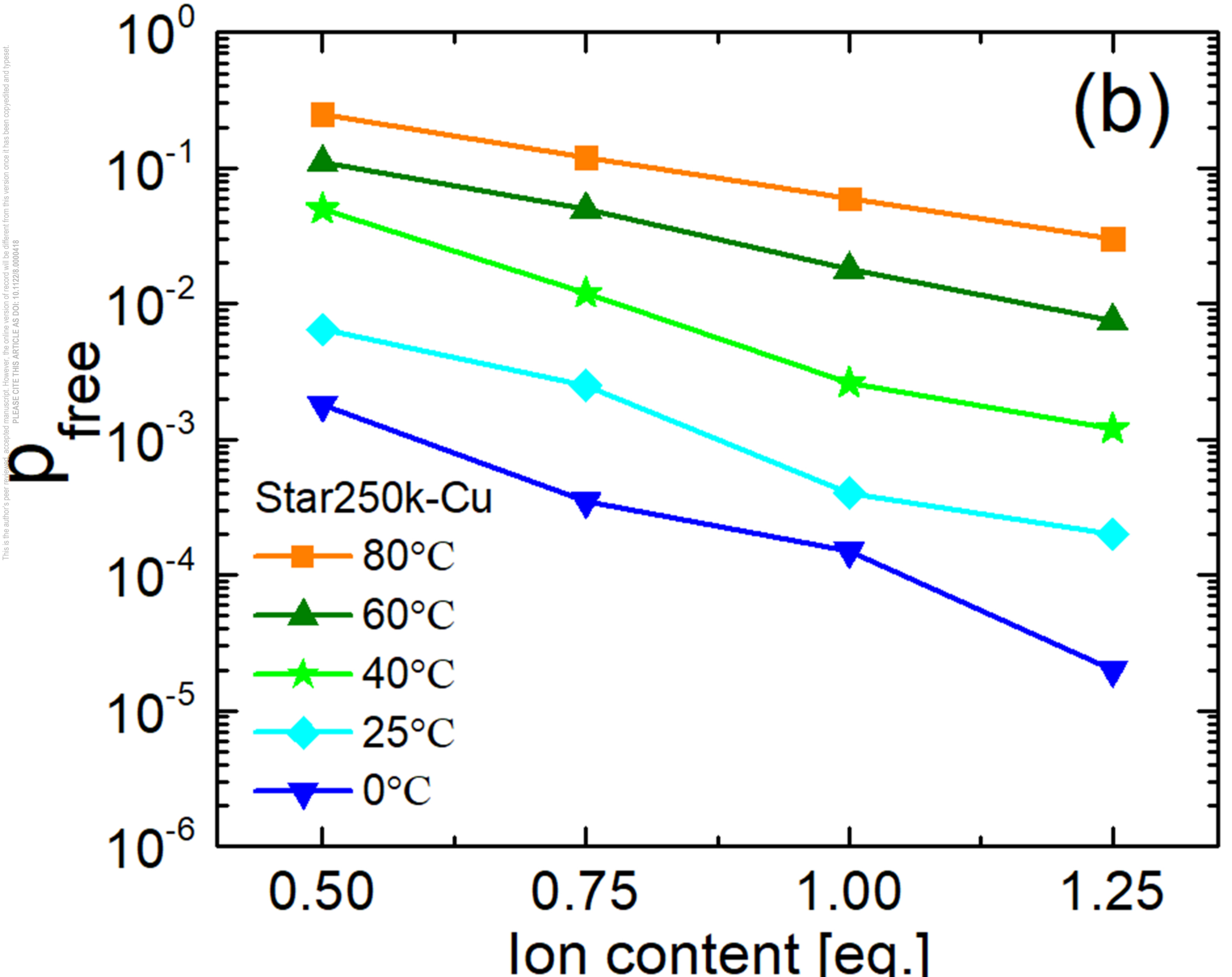

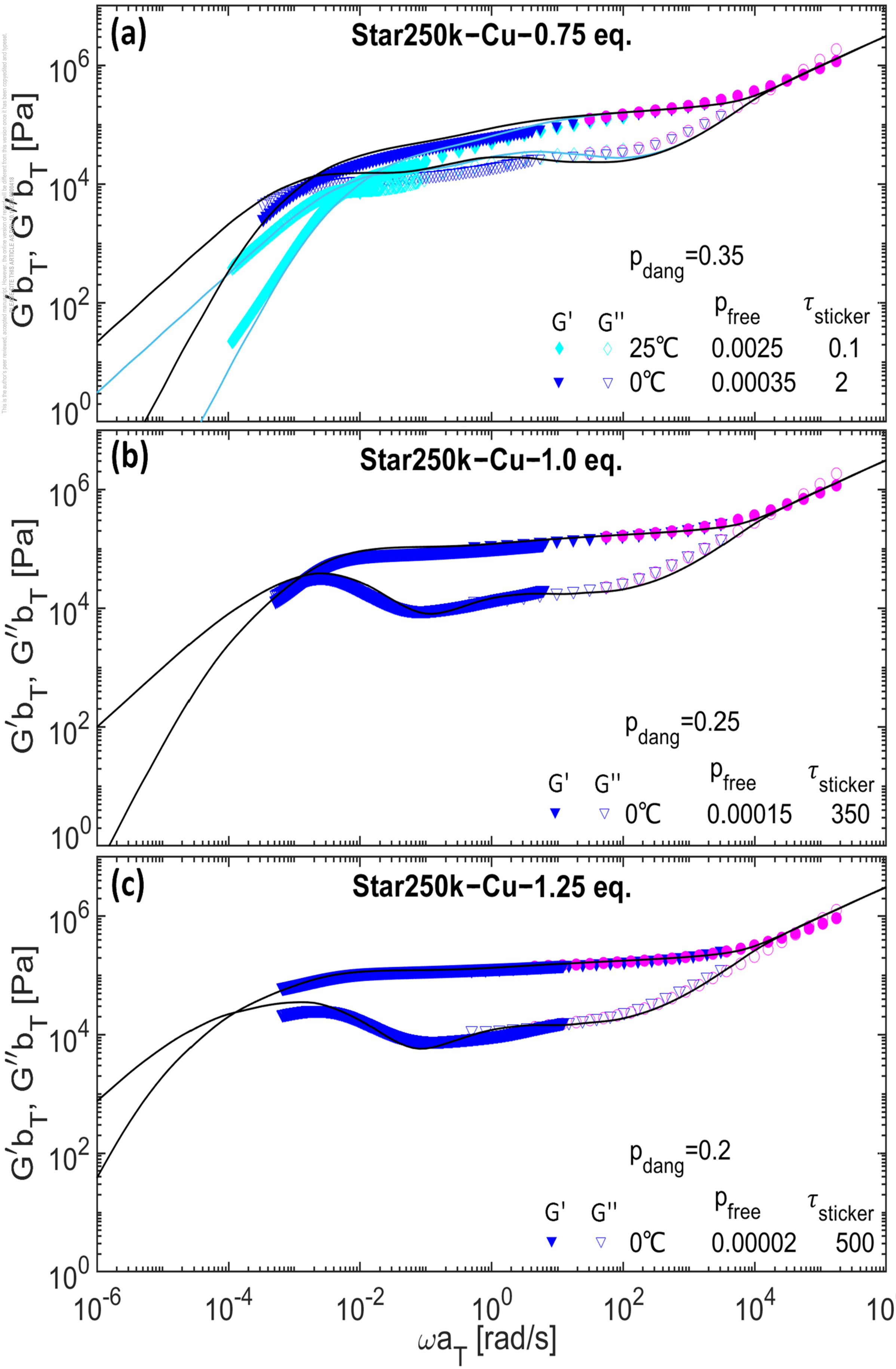

Journal of Rheology

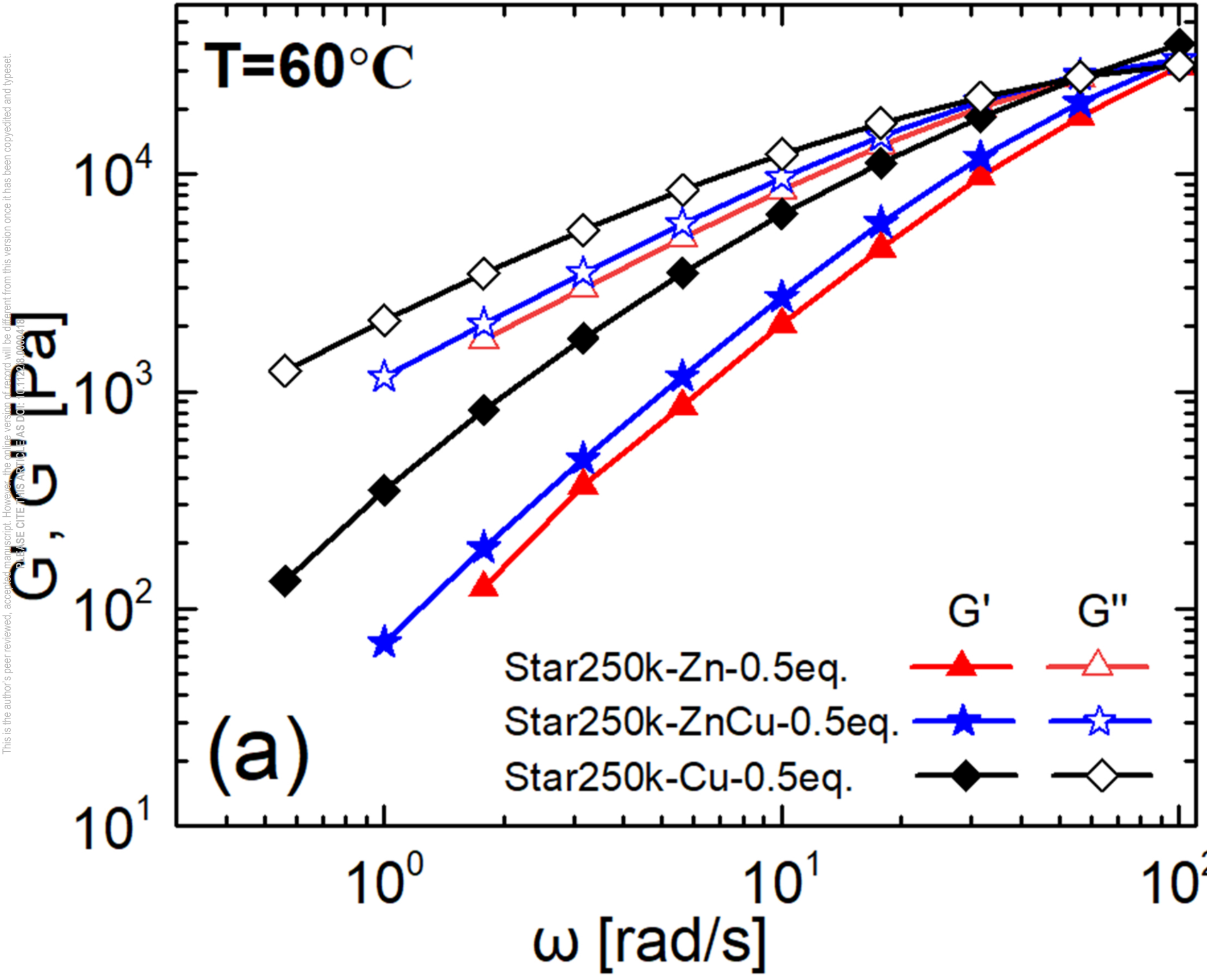

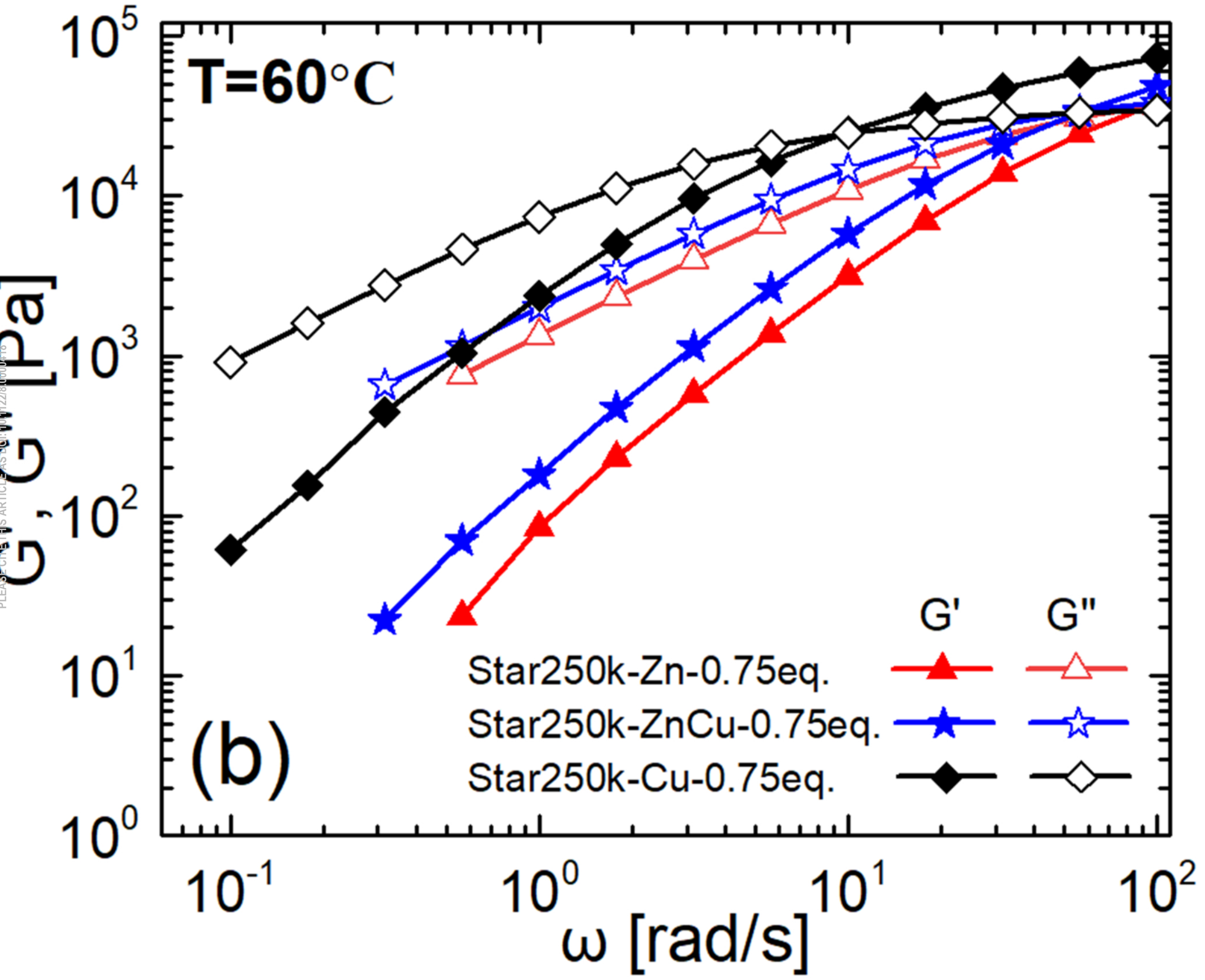

Journal of Rheology

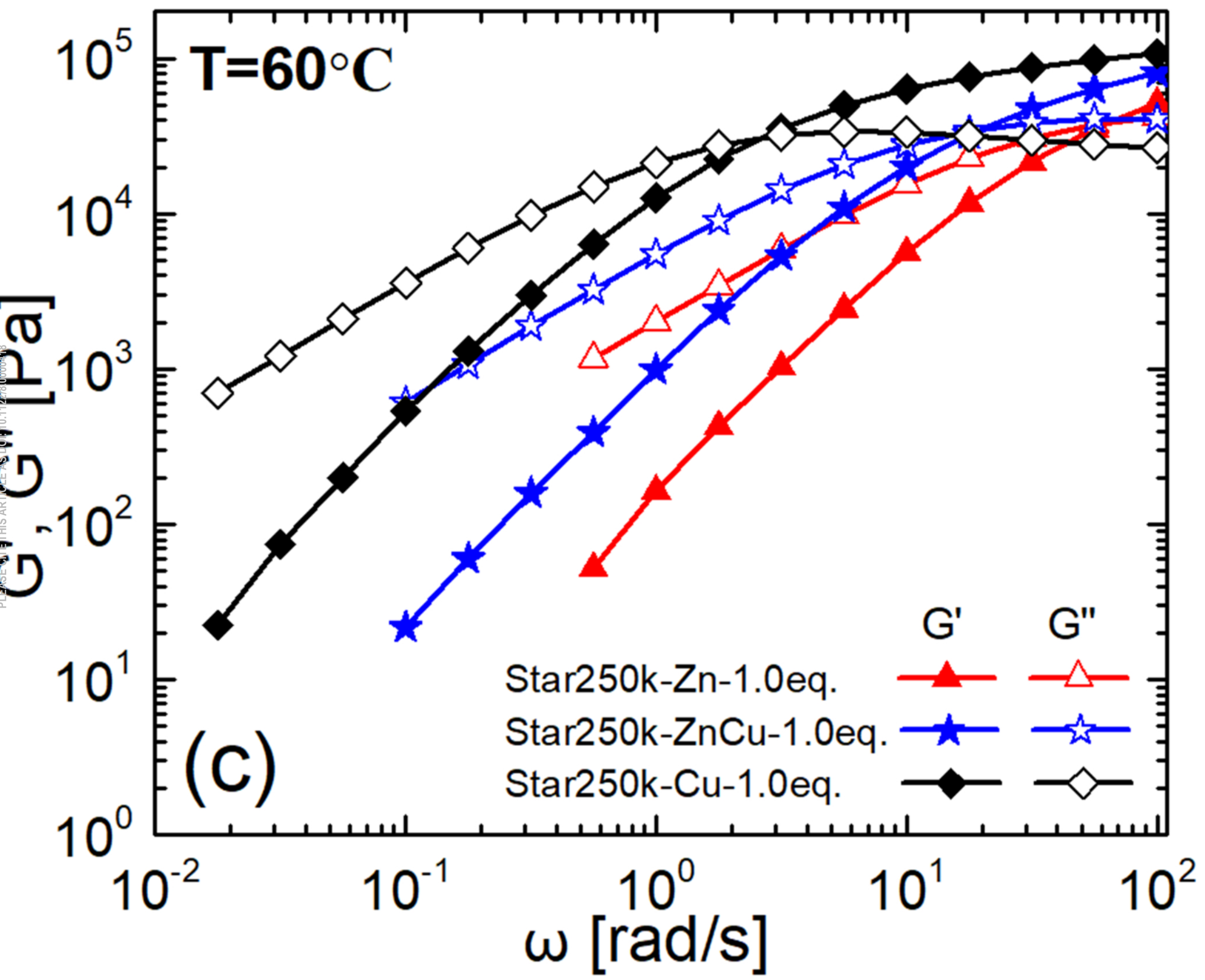

Journal of Rheology

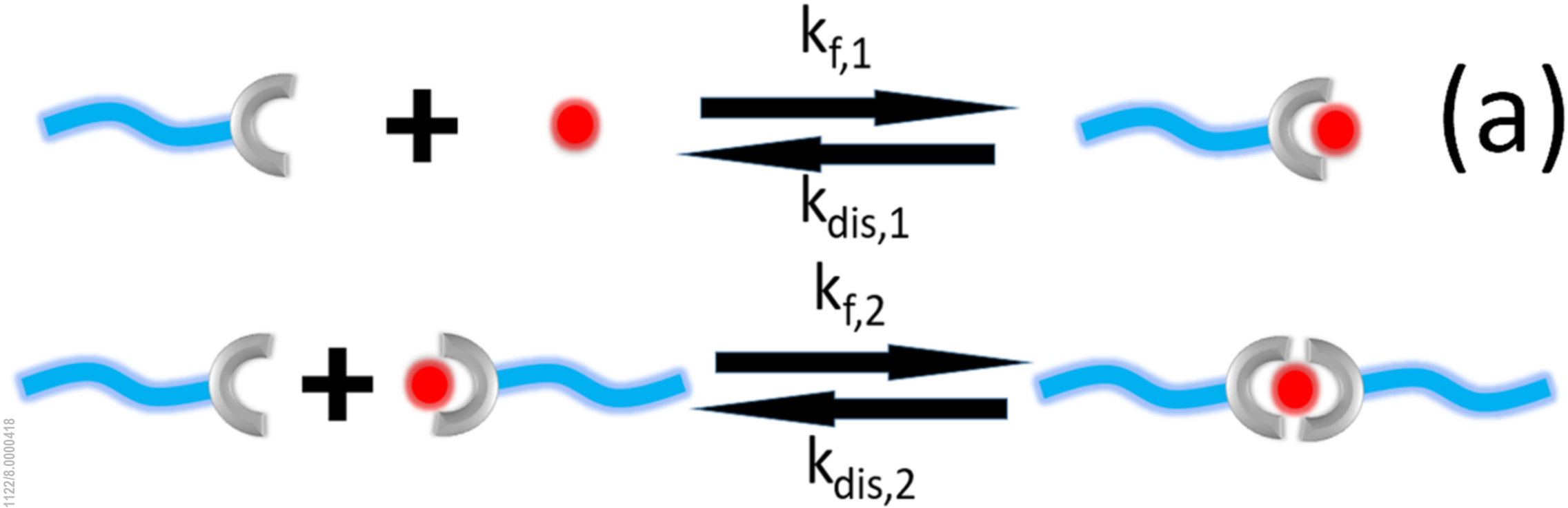

$$K_1 = k_{f,1}/k_{dis,1} \qquad K_2 = k_{f,2}/k_{dis,2} \qquad \beta = K_1 * K_2$$

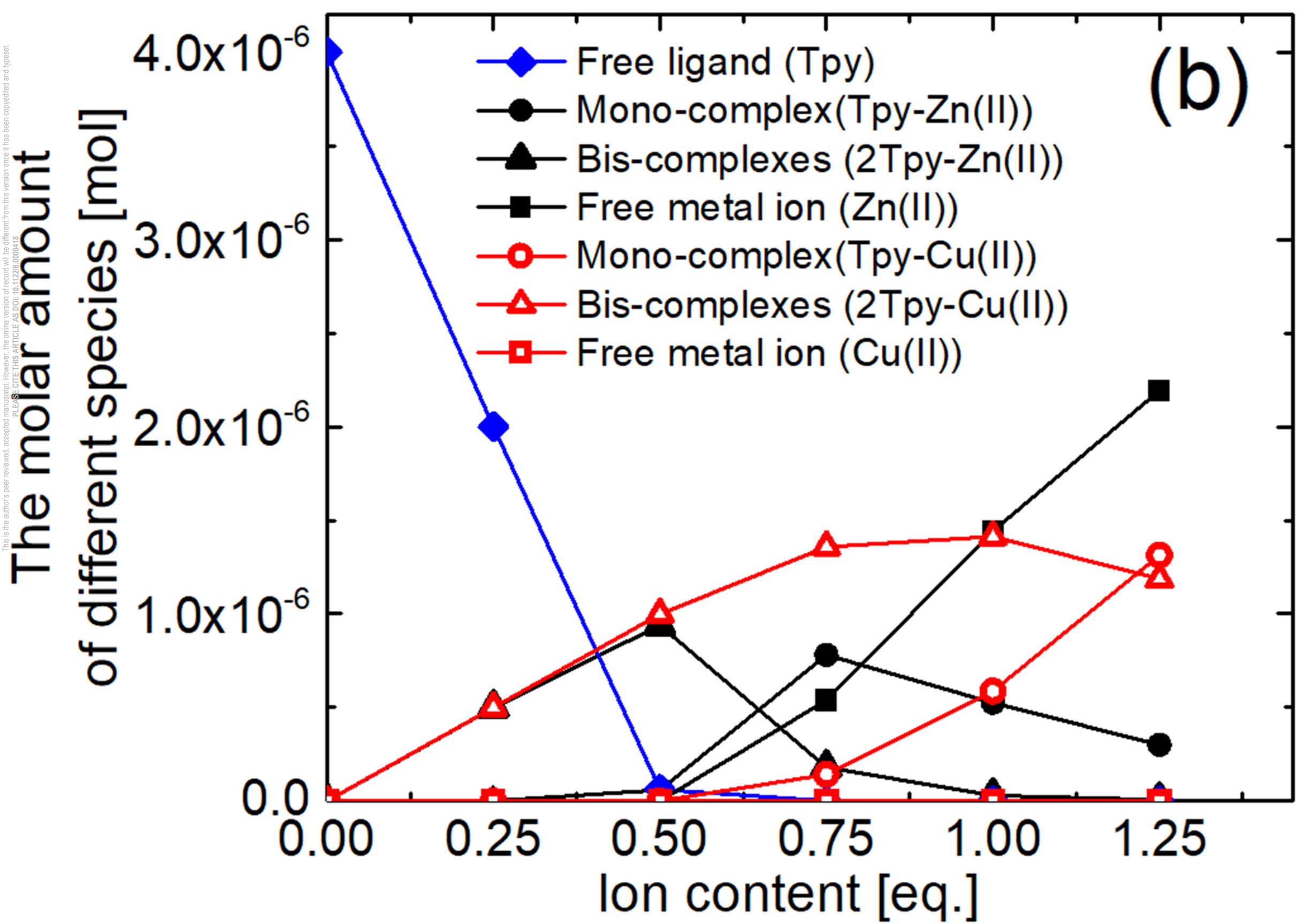

(a) Star250k−ZnCu−0.50 eq.

p_{dang}=0.5

G'	G''		p_{free}
■	□	80℃	0.7
▲	△	60℃	0.5
★	☆	40℃	0.3
♦	◇	25℃	0.16
▼	▽	0℃	0.09

(b) Star250k−ZnCu−0.75 eq.

p_{dang}=0.3

G'	G''		p_{free}
■	□	80℃	0.55
▲	△	60℃	0.37
★	☆	40℃	0.15
♦	◇	25℃	0.05
▼	▽	0℃	0.015

(c) Star250k−ZnCu−1.0 eq.

p_{dang}=0.2

G'	G''		p_{free}
■	□	80℃	0.3
▲	△	60℃	0.16
★	☆	40℃	0.06
♦	◇	25℃	0.01
▼	▽	0℃	0.0011

$G'b_T$, $G''b_T$ [Pa]

ωa_T [rad/s]